UNITED STATES DEPARTMENT OF THE INTERIOR

GEOLOGICAL SURVEY

Volcanic stratigraphy of part of McLendon volcano, Anderson mine area, Yavapai County, Arizona

By

William E. Brooks[1]

Open-File Report 84-350
1984

[1]Denver, Colorado

CONTENTS

ILLUSTRATIONS

TABLES

ABSTRACT

McLendon volcano is a large, 20-25 km diameter, mid-Tertiary stratovolcano located within the transition zone between the Colorado Plateau and the Basin and Range provinces. Lavas of the McLendon volcano are calc-alkaline with moderate K_2O, and were generated during subduction of the Farallon plate under southwestern North America. The greater portion of McLendon volcano is missing--either through erosion or caldera collapse.

Caldera collapse is evidenced by presence of possible outflow tuff, by mineralized sediments of possible moat-fill origin, and by a gravity low near the volcano. A 25-m.y. ash-flow tuff in the Harcuvar Mountains, 30 km south of McLendon volcano, may have come from the McLendon area. The tuff cannot be mapped into the McLendon area, but geochemical evidence, such as increasing U, Th, and Rb/Sr ratios, is suggestive that the ash-flow tuff is genetically related to McLendon volcano. Geochemical evidence is unclear, however, because the ash-flow tuff has been metasomatised. The tuff contains up to 12 percent K_2O and less than 1 percent Na_2O.

Sedimentary fill within the outline of the volcano is interpreted as moat sediments within the proposed McLendon caldera. A circular, -25 mgal gravity low, centered southwest of McLendon volcano, is dissimilar in shape, orientation, and intensity to basin-and-range-related gravity lows. The McLendon low could be the result of sediment infilling a caldera. Late Tertiary sediments at the Anderson mine contain uranium deposits interpreted as volcanogenic in origin.

Basin-and-range faulting has affected the 25-m.y.-old lavas of McLendon volcano but has not offset a 12-m.y. basalt flow that crops out to the northeast at Malpais Mesa. The effects of basin-and-range faulting are bracketed between 25 and 12 m.y. ago.

INTRODUCTION

This report describes the volcanic stratigraphy, field relations, petrography, and geochemistry of mafic to silicic lavas and volcaniclastic rocks that crop out as part of McLendon composite volcano located 70 km northwest of Wickenburg, Ariz. The mapped area, 100 km^2, is the remaining northeast flank of a large, mid-Tertiary volcano. The original dimensions are uncertain because most of the volcano is missing.

Access to the McLendon study area is from Arizona Highway 93 and unpaved ranch and mine roads. The closest urban center is Phoenix, Ariz., 190 km to the southeast. The town of Wickenburg is 65 km southeast of the study area.

Methods of study

The results presented in this report are based on 24 weeks of fieldwork during the fall and winter of 1977-78 and 1978-79. Mapping was done on Malpais Mesa SW (1:24,000), and portions of Malpais Mesa (1:24,000), and Date Creek Ranch NW Quadrangles (1:24,000). In highly jointed areas, structural detail was added through the use of aerial photographs.

Petrographic descriptions of the McLendon rocks are based on flat-stage examination of approximately 80 thin sections. Modal compositions were determined for 22 representative thin sections based on a traverse of 500 points (Van Der Plas and Tobi, 1965). Plagioclase compositions were determined on the maximum extinction angle of albite twins cut normal to (010), the Michel-Levy method.

Regional geology

The study area is within the poorly defined and somewhat arbitrary transition zone between the Arizona Basin and Range province to the southwest and the Colorado Plateau province to the northeast (fig. 1). This zone is wider in the southeast part of Arizona and narrows to the northwest. It is a rugged area, somewhat lower in elevation than the Colorado Plateau, and is cut by several valleys, the Chino, Tonto, and Verde, that were formed by downfaulting and erosion (Wilson, 1962). Exposures of generally flat-lying sedimentary rocks, that include limestone and quartzite of Ordovician age, and lavas ranging from basalt to rhyolite of Tertiary to Quaternary age predominate over the Precambrian granites, schists, and gneisses.

In Utah and northern Arizona the Colorado Plateau-Basin and Range boundary zone is well defined by high-angle, north-south-trending normal faults (Hamblin and Best, 1975), but its surface expression where the zone swings through southwestern Arizona is not as clear due to erosion and uplift. Geophysical measurements allow the extension of this conspicuous structural boundary of northwestern Arizona into the subsurface of southwestern Arizona: high heat flow (1.5-3.0 cal/cm^2) and a low magnetic profile in response to the thinner crust are typical of the Basin and Range (Blackwell, 1969; Chapman and others, 1978; Pakiser and Zeitz, 1965), as is the lesser crustal thickness for the Basin and Range (~20 km) when compared to the Colorado Plateau (~40 km) (fig. 2).

VOLCANIC STRATIGRAPHY

Mafic lavas, volcaniclastic rocks, and silicic lavas make up the McLendon volcano. In the northeast part of the map area is a flat-lying basalt of uncertain relationship to McLendon volcano, but whose distribution and attitude has structural and tectonic significance. Locations for analyzed samples are listed in Appendix A.

Mafic lavas

The basal volcanic rocks of McLendon volcano are basalts and andesites exposed over an area of 25 km^2 in the southern portion of the map area and to a lesser extent to the north adjacent to the Santa Maria River (fig. 3). These rocks are nonconformable upon Precambrian rocks and, as a unit, are disconformable with overlying volcaniclastic rocks. At a few places, andesite intertongues with overlying volcaniclastic rocks. The lavas are not exposed in an orderly stratigraphic section, which suggests that the flows are not laterally continuous. The composite thickness of basalt and andesite is approximately 75 m.

Weathered outcrop colors range from red brown to purple, and flow contacts are usually marked by an oxidized, vesicular flow top in contact with the basal breccia of the overlying flow. Internal flow features, such as alined phenocrysts and inclined pipe vesicles, are rare or absent.

Water-free silica values range from 48.9 to 49.1 percent for the basalts and from 56.6 to 60.8 percent for the andesites. Within each chemical classification are distinct petrographic types (table 1).

Basalts

Basaltic lavas (table 1) of undetermined volume represent the initial eruptive phase of McLendon volcano. Although most basalt is older than the andesite, remnants of a basaltic spatter cone near Tres Alamos Spring, southwest portion of the geologic map, that is younger than the andesite indicate that basaltic activity also took place after eruption of andesite.

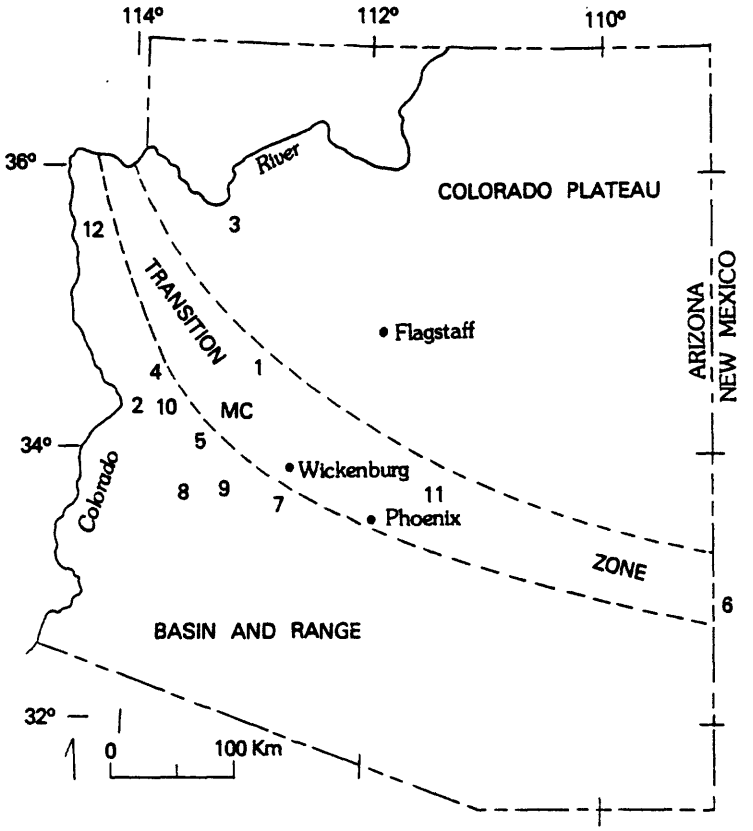

Figure 1.--Location map for study area (MC-McLendon volcano) and other areas cited in text.

1--Bagdad Copper deposit	Baker and Clayton, 1970
2--Whipple, Buckskin Mtns.	G. A. Davis and others, 1977
3--Peach Springs Tuff	Fuis, 1974
4--Artillery Mountains	Lasky and Webber, 1949
5--Anderson Mine	Otton, 1977
6--Mogollon-Datil volcanic field	Ratté and Grotbo, 1979
7--Vulture Mountains	Rehrig and others, 1980
8--Harquavar Mtns.	Rehrig and Reynolds, 1977
9--Huarquahalla Mtns.	Rehrig and others, 1980
10--Rawhide Mtns.	Shackleford, 1976
11--Superior volcanic field	Sheridan and others, 1970
12--Oatman district	Thorson, 1971

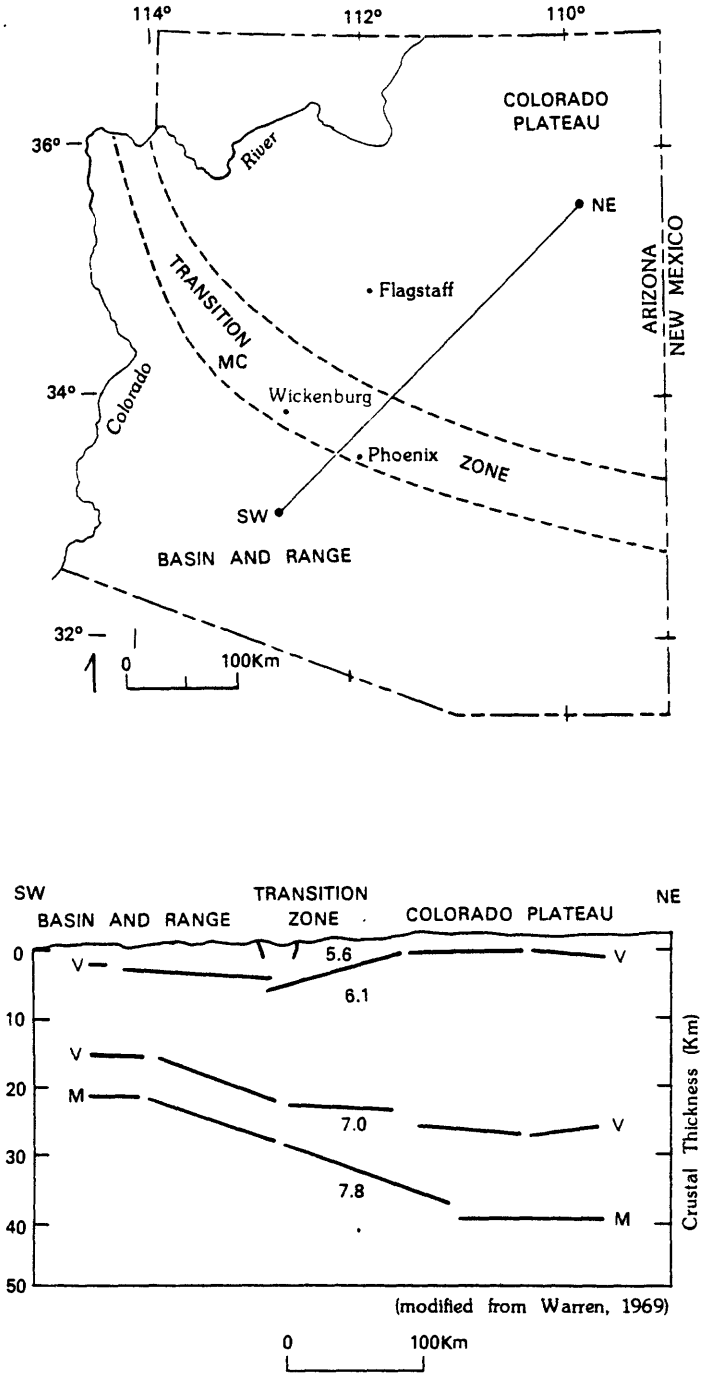

Figure 2.--Index map and cross section showing relationship of transition zone to crustal structure in southwestern Arizona. (MC - McLendon volcano; M - Mohorovicic discontinuity; V - seismic velocity zone boundary; seismic velocity in km/sec.)

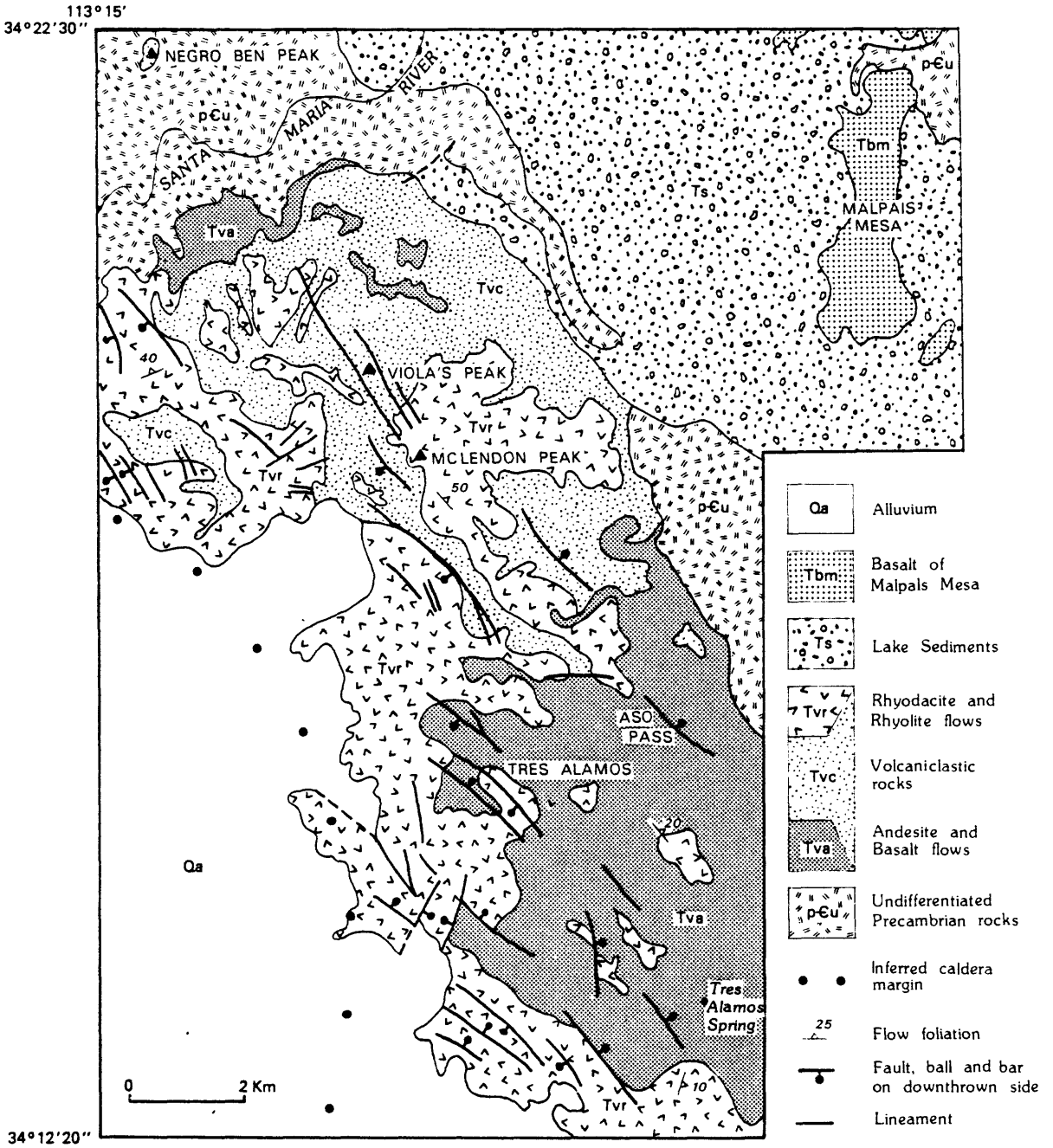

Figure 3.--Generalized geologic map of part of McLendon volcano, Yavapai County, Arizona.

Aphanitic flows

In hand sample the aphanitic basalt is black and dense. In thin section plagioclase is the most abundant mineral phase with 0.2 mm microlites in a meshwork. Twinned crystals (An_{50-70}) are more common than zoned microlites. Olivine occurs as grains (~0.05 mm) and in clots up to 1.0 mm in diameter. Alteration has cloaked the olivine with an exterior rim of iddingsite and a serpentine-like mineral stained with hematite. Unaltered grains are euhedral to subhedral with a 2V of approximately 80^{o} indicative of Mg-rich olivine (Deer and others, 1966, p. 6). Clinopyroxene with weak hourglass extinction and concentric zoning indicates titanaugite (Deer and others, 1966, p. 120), even though the typical purple-brown pleochroism is not apparent. The moderate to low 2V, octagonal cross section, and distinctive zoning are typical of augite. Reddish-brown glass with blebs of hematite is contained in the groundmass. Euhedral magnetite is abundant.

To the north, near the Santa Maria River, a chemically similar basalt crops out. Phenocrysts of plagioclase are absent, but plagioclase microlites (An_{54-60}) are present as a pilotaxitic groundmass and host 0.25 to 1.0 mm clots and phenocrysts of olivine and pyroxene. Olivine has a high 2V (~90^{o}), and some phenocrysts have irregular disequilibrium cores. Augite is present and shows faint concentric zoning. Biotite is present as sparse splinters (0.01-0.03 mm) with birdseye extinction and deep-brown pleochroism. The occurrence of biotite in basalts is rare but not unusual (Deer and others, 1966, p. 213).

Medium-phaneritic flows

Irregular exposures of a medium-phaneritic basalt occur near Tres Alamos Spring and at Aso Pass in the southeastern part of the map area. Phenocrysts of plagioclase up to 2.0 mm are abundant, giving the rocks a plutonic appearance (table 1, sample 205-79).

Contacts between phaneritic basalt and aphanitic basalt at Tres Alamos Spring are gradational. Oxidized flow breccias and pyroclastic debris, including bombs and bomb fragments (~30 cm), are associated with the phanerite. A gradation in crystal size from the vent outward indicates that the phanerite near Tres Alamos Spring is the ponded, throat lava of a small satellitic vent. A similar interpretation is reasonable for the phanerite at Aso Pass.

Plagioclase phenocrysts range in size from 0.5 to 2.0 mm and are intermediate in composition (An_{44-64}). Twinned and normally zoned crystals occur individually or in glomeroporphyritic clots with olivine. The presence of resorption cavities and scattered glass blebs indicates changing magma composition or equilibrium adjustments, in response to changing pressures resulting from ascent of the magma.

Olivine phenocrysts are euhedral and average 1.0 mm in diameter. Faint cleavage traces and cracks are present in the high-Mg olivine. Iddingsite occurs as an alteration product partially or totally enclosing the olivine or as an amorphous interstitial residue.

Andesites

Andesitic lavas exposed over an area of approximately 25 km^2 were erupted after basalt (fig. 3). Eruption of the basalt and andesite was close in time, with andesite appearing to be more voluminous.

Table 1.--Analyses of mafic lavas from McLendon volcano, Yavapai County, Ariz.

[Method as described under "single solution" in U.S. Geological Survey Bulletin 1401; analysts, H. R. Smith and J. E. Reid]

	Basalts			Andesites			
Field No.	204-79	205-79	212-79	203-79	137-77	177-78	211-79
Lab. No.	W-205353	W-205354	W-205356	W-205352	W-200281	W-201666	W-205355
	aphanitic	medium-phaneritic	aphanitic	medium-phaneritic	seriate-porphyritic	quartz-bearing	quartz-bearing
Major oxides (weight percent), recalculated without H_2O and CO_2							
SiO_2	49.1	48.9	49.1	60.8	58.4	56.6	59.9
Al_2O_3	15.8	17.3	15.8	16.8	17.1	17.5	16.8
Fe_2O_3	7.4	8.6	4.4	5.0	4.0	7.0	5.4
FeO	2.8	2.1	4.8	.5	2.2	.4	.8
MgO	7.2	5.8	8.8	2.6	3.7	2.7	2.9
CaO	11.4	10.8	10.9	5.5	7.1	5.6	6.2
Na_2O	3.3	3.3	3.1	4.0	3.8	4.3	4.0
K_2O	1.0	1.1	1.3	3.6	2.5	3.5	2.8
TiO_2	1.3	1.4	1.1	.8	.9	1.4	.9
P_2O_5	.6	.5	.5	.3	.2	.9	.2
MnO	.1	.2	.2	.1	.1	.1	.1
TOTALS	100.0	100.0	100.0	100.0	100.0	100.0	100.0
H_2O+	1.5	1.4	1.9	1.2	1.0	.5	1.1
H_2O-	.7	.9	.5	1.4	.9	1.4	1.3
CO_2	.1	.3	---	---	---	.1	---
Norms (weight percent)							
Quartz	---	0.1	---	10.5	9.2	5.7	11.3
Corundum	---	---	---	---	---	---	---
Orthoclase	6.0	6.7	6.8	21.4	15.0	20.7	16.3
Albite	27.6	27.8	22.3	34.1	31.8	36.7	33.8
Anorthite	25.2	29.0	21.5	17.5	22.2	18.3	19.5
Di-Wollastonite	11.0	7.9	9.0	3.2	4.8	1.5	4.1
Di-Enstatite	9.5	6.8	6.9	2.8	4.1	1.3	3.6
Di-Ferrosilite	---	---	1.2	---	---	---	---
Hy-Enstatite	4.4	7.5	11.9	3.7	5.0	5.4	3.6
Hy-Ferrosilite	---	---	2.0	---	---	---	---
Ol-Fosterite	2.8	---	8.4	---	---	---	---
Ol-Fayalite	---	---	1.5	---	---	---	---
Magnetite	5.4	3.0	5.5	---	4.9	---	.4
Hematite	3.6	6.5	---	5.0	.6	7.0	5.2
Ilmenite	2.5	2.7	1.8	1.2	1.7	1.2	1.7
Apatite	1.5	1.3	1.1	.7	.5	2.1	.6
Calcite	.3	.8	.1	---	.1	.2	---
Phenocrysts (volume percent)							
Plagioclase	---	71.1	---	21.1	42.2	51.4	63.0
microlites	47.0	---	51.8	47.3	---	---	---
Olivine	32.0	14.9	19.8	---	8.2	---	5.6
iddingsite	---	10.6	---	---	4.6	---	9.0
antigorite	---	---	---	13.2	---	12.6	---
Clinopyroxene	1.6	---	8.2	.4	7.0	2.6	9.0
Oxyhornblende	---	---	---	---	2.8	3.4	---
Biotite	---	1.6	1.0	---	---	---	---
Opaques	16.8	1.8	19.2	16.8	15.2	28.8	12.4
Groundmass	2.6	---	---	1.2	20.0	1.0	---
Quartz (xenocrystic)	---	---	---	---	---	.2	1.0
TOTALS	100.0	100.0	100.0	100.0	100.0	100.0	100.0

Medium-phaneritic flows

The medium-phaneritic andesite weathers tan to brown, and oxidized minerals give the rock a spotty appearance. Plagioclase is abundant as phenocrysts (2.0 mm), as flow-alined microlites, and in clots with mafic minerals. A serpentine-like mineral is present as an alteration product of olivine (Deer and others, 1966, p. 5). Unaltered olivine is rarely present, but the abundance of the alteration product suggests that olivine was as much as 10 percent of the original modal composition. Clinopyroxene is present in trace amounts in the groundmass and one or two grains are as large as 0.5 mm. Magnetite is abundant in the microlite-crystallite-rich groundmass.

Seriate-porphyritic flows

This andesite is dark gray to black and has ruddy oxidation staining along joint and fracture surfaces. Plagioclase microlites and 2.0 mm phenocrysts (An_{40-65}) are present. Plagioclase is occasionally glomeroporphyritic with olivine. Resorption has reduced some phenocrysts to skeletal outlines while only partially attacking the interiors of other crystals. Normally zoned and twinned crystals are common and both show disequilibrium textures.

Alteration of the olivine to finely granular iddingsite gives the thin section an overall reddish appearance. A serpentine-like mineral is pseudomorphic after olivine (0.03-0.5 mm), and together they comprise approximately 12 percent of the mode. This alteration is possible in low to moderate temperature systems (~400° C) with the addition of H_2O and SiO_2 (Deer and others, 1966, p. 5). An active volcanic environment would mobilize and provide these oxides.

Twinned clinopyroxene with an oxidation halo is present. Hornblende (0.25-1.0 mm) is altered to dark-red oxyhornblende and could easily be confused with iddingsite if the amphibole cleavage were obscured. Euhedral magnetite is abundant throughout the brown-green groundmass.

Quartz-bearing flows

A distinctive quartz-bearing andesite, of limited areal extent, crops out in the northwestern part of the study area, and is accessible from the Santa Maria River. Plagioclase (An_{35-55}) is abundant as crystals that rarely exceed 1.0 mm in length. Twinned microlites are generally less than 0.45 mm in length. A concentric zone of glassy inclusions is present as a thin ring and both patchy and normal zoning are present.

Quartz is present as polycrystalline xenocrysts that are from 0.50 to 1.0 mm in diameter. Quartz xenocrysts have thin reaction rims of pyroxene and total one percent or less of the mode.

Most olivine is altered to iddingsite or through thermal alteration to a fibrous, netlike pseudomorph. The skeletal outline is the best evidence for the former presence of olivine. Thoroughly oxidized hornblende and minor clinopyroxene total almost 6 percent of the minerals present with euhedral magnetite and sparse ilmenite totalling approximately 30 percent.

Volcaniclastic rocks

The term "volcaniclastic rocks" includes the entire spectrum of fragmental rocks formed by any volcanic mechanism and mixed with subordinate amounts of nonvolcanic fragments (Fisher, 1961, 1966b). This broad category includes:

1. Epiclastic rocks that are formed from previously deposited volcanic rocks with an appreciable interval between deposition of the original volcanic pile and subsequent erosion, reworking, and deposition (Pettijohn, 1975, p. 313).
2. Pyroclastic rocks that are produced by explosion or aerial ejection of material from a volcanic vent (Pettijohn, 1975, p. 298) or generated by disruption as a direct result of volcanic action (Schmid, 1981). This term may be further subdivided into primary and secondary pyroclastic rocks, both of which may contain pumice. Primary pyroclastic rocks include ash-fall, ash-flow, and base-surge deposits. Secondary pyroclastic rocks have been remobilized by water soon after initial deposition and include lahars and mudflows. Field and petrographic evidence for reworking includes imbricated biotites, rounding of sand-sized grains (crystal as well as lithic fragments), graded bedding, a clast-supported matrix of sand and smaller sized particles, and crossbeds. The absence of bomb-sag features indicates that deposition occurred in a water-dominant environment (Williams and McBirney, 1979, p. 137).

Lower volcaniclastic rocks

The lower volcaniclastic rocks of the study area are primary and include several rhyolitic ash-flow tuffs (2-3 m thick) exposed in the southern part of the area (fig. 3). Shards, 1.0 mm plagioclase, and quartz phenocrysts are visible in hand sample. Density is variable, reflecting poorly welded to welded zones. In thin section the rock is vitroclastic, and has 15 percent crystals in a glassy matrix composed of cuspate, bubble-wall shards and compressed, eutaxitic pumice. Crystals include plagioclase, minor quartz, and lesser amounts of biotite, sanidine, altered pyroxene, and opaque minerals. The anomalously high silica content of these tuffs (see below) suggests secondary silicification. Water-free major oxides (weight percent) for a single sample (E-219-81) are:

SiO_2---	82.4
Al_2O_3--	9.4
$FeTO_3$--	1.1
MgO----	0.2
CaO----	0.3
Na_2O---	2.7
K_2O----	3.8
TiO_2---	0.1
P_2O_5---	<0.05 (rounded to 0)
MnO----	0.04 (rounded to 0)
TOTAL--	100.0
LOI----	1.2

(Analysis by X-ray spectroscopy; analysts: J. S. Wahlberg, J. E. Taggart, and J. W. Baker; $FeTO_3$ indicates total iron reported as Fe_2O_3.)

Upper volcaniclastic rocks

The upper volcaniclastic rocks include primary and secondary pyroclastic facies. Massive secondary beds, with boulders 3-5 m in diameter, interfinger with thin beds of ash-fall lapilli tuff 3-4 cm thick. The unit has lateral continuity, but the fine-grained ash-fall tuff cannot be mapped for any great distance. The upper volcaniclastic rocks are 350-400 m thick and are exposed over 35 km^2.

East-dipping attitudes measured at flow/volcaniclastic contacts are field evidence (Compton, 1962, p. 264) for the westward location of the central vent of McLendon volcano, assuming no post-eruptive tilting of beds. Strike patterns are concentric, while dips are generally radial to the north and northeast.

The upper volcaniclastic rocks are buff to tan, and the incorporated clasts of rhyodacite are shades of red and gray. Most clasts are rhyodacite, but a mixture of metamorphic and andesitic clasts is present where slurry-like, reworked beds overlie dominantly metamorphic and andesitic terranes. Lubricating water may have come from a crater lake that had occupied McLendon volcano, or, more likely, from rain generated during plinian seeding of the atmosphere with ash.

Sedimentary petrology

Terms such as "lahar" and "mudflow" are applicable in a general description of the volcaniclastic rocks. Field evidence that indicates deposition by an aqueous system includes reverse and normal grading that indicate a change in velocity and water content of the mudflow (Schminke, 1967). Sand-sized particles are poorly sorted and are subrounded to angular. Also, imbrication of biotites indicates a depositional environment sensitive to gravity and current (Potter and Pettijohn, 1977, p. 33).

The upper volcaniclastic sediments are petrographically defined in terms of three components: glass, including shards; crystals, including whole and broken crystals that are not part of rock fragments; and metamorphic or volcanic lithics. Percentages of these three components allow classification into vitric, lithic (volcanic or metamorphic), or crystal tuff (fig. 4).

The crystal component is chiefly broken oxyhornblende (~0.25 mm), zoned plagioclase, and oxybiotite. The plagioclase (~0.25 mm) is approximately An_{40} and similar in composition to the plagioclase of the overlying rhyodacite.

The Precambrian terrane underlying McLendon volcano is the source for the 2.0 mm metamorphic rock fragments that contain polycrystalline quartz, muscovite, myrmekite, and tartan-twinned potassium feldspars. The volume of metamorphic and volcanic lithic fragments varies from outcrop to outcrop depending on the stratigraphic location above metamorphic or volcanic terrane.

Mosaic granophyre resulting from devitrification indicates the former abundance of glass shards. The presence of tube-vesicle and bubble-wall shards demonstrates that the fragments were generated from a gas-charged and explosive magma (Heiken, 1972). Cold emplacement of the volcaniclastic rocks is indicated by the noncompressed, nonwelded, and unoriented attitude of shards and pumice. The volcaniclastic rocks are cemented by clay and chalcedony. Clay may be primary, due to hydration and decomposition of some glass shards. Later, iron-stained chalcedony precipitated in a pore-filling, radial pattern.

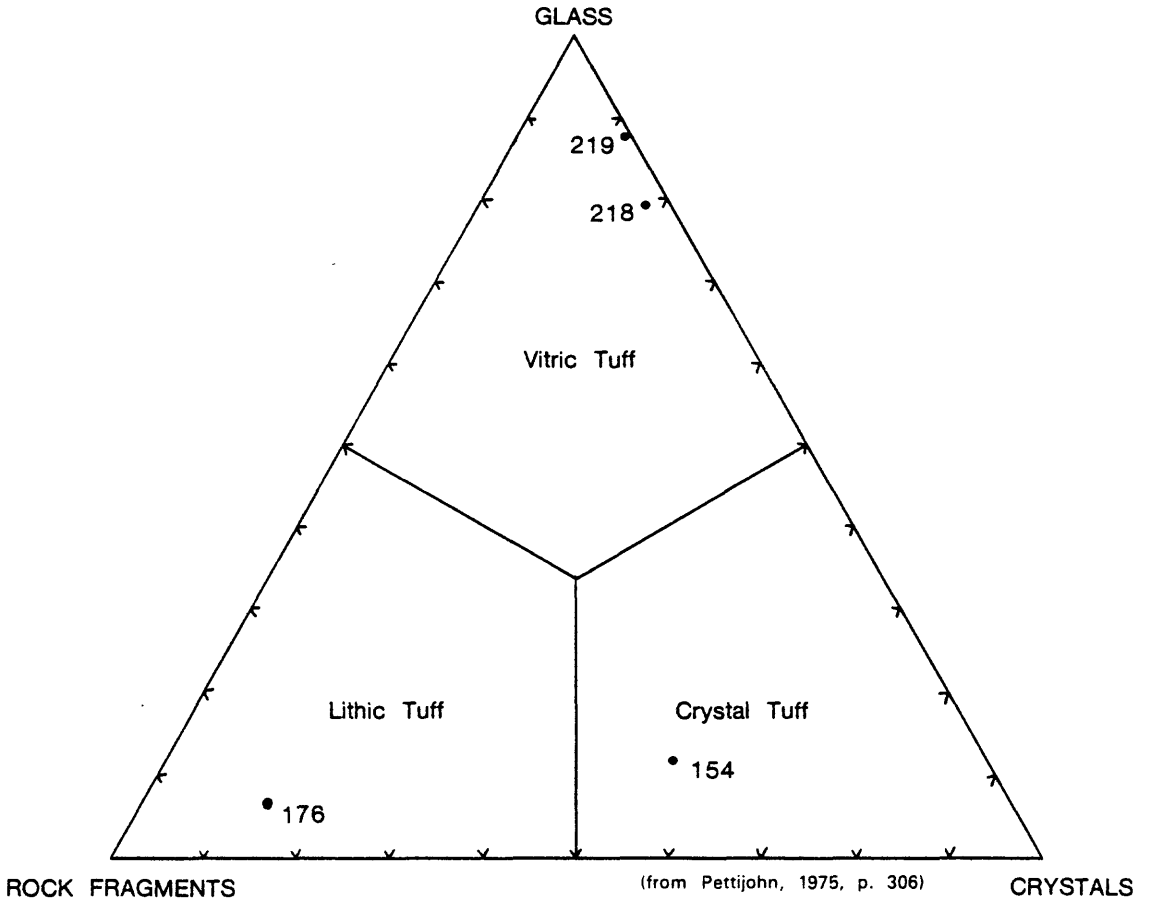

	primary pyroclastics		secondary pyroclastics	
Sample Number	218-81	219-81	154-77	176-78
Rock fragments:	1.8	--	33.4	--
volcanic-----	--	--	--	11.3
metamorphic--	--	--	--	68.8
Glass----------	79.6	87.0	11.8	6.3
Crystals-------	18.6	13.0	54.8	13.6
TOTAL-----	100.0	100.0	100.0	100.0

Figure 4.--Modal analyses and classification of volcaniclastic rocks, McLendon volcano, Yavapai County, Ariz.

Silicic lavas

Rhyodacite and low-silica rhyolite lavas unconformably overlie the volcaniclastic rocks. The flows cover 30 km^2 and have a composite thickness of 150 m with some individual, valley-filling flows as thick as 150 m. The areal extent of low-silica rhyolite is far less than that of the rhyodacite. In table 2, water-free silica values range from 65.9 to 73.2 percent and indicate a rhyodacite field, 65 to 70 percent SiO_2, and a low-silica rhyolite field, 70 to 73 percent SiO_2. Classification by the Church (1975) method is discussed in a later chapter.

In general, the silicic flows have a brecciated or banded basal vitrophyre that is transitional into foliated flow interior. The carapace is poorly exposed but appears rubbly and oxidized in outcrops where younger flows have been eroded or were not emplaced.

At Tres Alamos a 75 m rhyodacite flow is exposed. The lower 4 to 5 m has a hackly, poker-chip appearance with polygonal wedges 10-20 cm in diameter and approximately 5 cm thick. This lower zone passes into massive flow interior which appears as a crude, irregular colonnade 20 m thick. The reddened and brecciated carapace is overlain by bedded, primary pyroclastic rocks no more than several meters thick.

The common subparallel orientation of plagioclase phenocrysts in the rhyodacite and alinement of compaction foliation permits mapping of flow structures. Ramps are common and are thought due to a topographic barrier that impeded the advancing lava (Christiansen and Lipman, 1966) in a style similar to glacial advance over a riegel (Reineck and Singh, 1975, p. 164). Flow foliations are inclined and, in some cases, vertical. From a distance these tablets (45 cm x 20 cm x 5 cm) have the appearance of rakishly alined tombstones. Examination of hand samples indicates that these rocks could be mapped as a unit based on the occurrence of plagioclase, hornblende, and biotite.

The rhyodacite map unit can be subdivided on the basis of petrography and rock chemistry. Three petrographic types are present: (1) mafic-rich (hornblende, ± biotite, ± augite, ± hypersthene), (2) quartz-bearing (xenocrystic), and (3) two-pyroxene (greater than one percent modal orthopyroxene) (table 2).

Age of the rhyodacite is 24.7±0.4 m.y. based on a single K-Ar date on a plagioclase separate (Neil Suneson, written commun., 1978).

Mafic-rich rhyodacite

The mafic-rich rhyodacite is gray to reddish gray, porphyritic with plagioclase, hornblende, and biotite. Maximum thickness is approximately 180 m near McLendon Peak, and this lava overlies the thick volcaniclastic section.

Hornblende is present in almost all flows, but varying amounts of biotite, orthopyroxene, and clinopyroxene are present. The range in silica content for this rhyodacite subgroup is from 65.9 to 69.3 percent. Phenocrysts of plagioclase average 2.0 mm, while cumulocrysts with amphibole may be as large as 4.0 mm. Twinned laths (An_{40-60}) are more abundant than normally zoned crystals. Rare, reversely zoned crystals are smaller (~0.1 mm) than the normally zoned crystals (~0.5 mm). Disequilibrium is indicated by embayments and vermicular resorption along the margins of most grains. Some interior resorption cavities have developed.

Table 2.--Analyses of silicic lavas from McLendon volcano, Yavapai County, Ariz.

[Method as described under "single solution" in U.S. Geological Survey Bulletin 1401; analysts, H. R. Smith and J. E. Reid]

	Rhyodacites						Low-Silica Rhyolite			
Field No.	132 -77	156 -78	167 -78	149 -78	174 -78	171 -78	145 -78	166 -78	169 -78	170 -78
Lab. No.	W-20 0279	W-20 1655	W-20 1658	W-20 1654	W-20 1664	W-20 1661	W-20 0282	W-20 1657	W-20 1659	W-20 1660
	mafic	mafic	mafic	quartz-bearing	quartz-bearing	two-pyroxene	felsite	felsite	felsite	felsite [c]
Major oxides (weight percent), recalculated without H_2O and CO_2										
SiO_2	66.0	65.9	69.3	68.0	69.0	69.8	70.2	70.8	70.8	73.2
Al_2O_3	16.2	16.4	15.7	15.5	15.0	15.7	15.1	15.2	14.8	14.9
Fe_2O_3	1.7	3.6	1.6	3.2	2.6	1.4	1.8	1.4	1.7	1.3
FeO	1.9	.4	1.0	.2	.5	1.2	1.0	.8	.7	---
MgO	1.6	1.6	.9	1.3	.9	1.2	1.1	.8	1.0	.3
CaO	3.7	3.9	2.6	3.4	2.1	2.4	2.6	2.6	2.7	1.5
Na_2O	4.4	4.1	4.3	4.2	3.3	3.7	3.9	3.9	3.8	4.2
K_2O	3.6	3.4	3.9	3.4	5.9	3.9	3.7	4.0	3.9	4.3
TiO_2	.6	.5	.4	.5	.4	.4	.4	.3	.3	.2
P_2O_5	.2	.2	.2	.2	.2	.2	.1	.1	.2	.1
MnO	.1	---	.1	.1	.1	.1	.1	.1	.1	---
TOTAL	100.0	100.0	100.0	100.0	100.0	100.0	100.0	100.0	100.0	100.0
H_2O+	1.5	---	1.4	.2	.1	1.2	2.1	2.0	---	.2
H_2O-	.3	.9	.3	1.2	.4	.6	.3	.8	.3	.3
CO_2	---	---	---	---	.2	---	---	---	---	---
Norms (weight percent)										
Quartz	17.0	19.3	23.2	22.5	22.8	27.0	26.5	26.5	26.9	29.0
Corundum	---	---	.2	---	.4	1.6	.3	---	---	.8
Orthoclase	21.2	20.4	23.0	19.9	34.8	23.0	21.9	23.7	23.2	25.5
Albite	37.3	34.4	36.4	35.3	27.5	31.2	33.1	33.0	32.3	35.7
Anorthite	13.5	16.2	11.4	14.4	7.6	10.2	11.9	11.7	11.6	6.6
Di-Wollastonite	.3	.5	---	.3	---	---	---	---	.3	---
Di-Enstatite	.9	.4	---	.3	---	---	---	---	.2	---
Di-Ferrosilite	.3	---	---	---	---	---	---	---	---	---
Hy-Enstatite	3.2	3.6	2.2	3.0	2.3	3.1	2.8	2.0	2.2	.6
Hy-Ferrosilite	1.0	---	---	---	---	.5	---	---	---	---
Ol-Fosterite	---	---	---	---	---	---	---	---	---	---
Ol-Fayalite	---	---	---	---	---	---	---	---	---	---
Magnetite	2.5	---	2.3	---	.6	2.1	2.2	1.8	1.5	---
Hematite	---	3.6	---	3.2	2.1	---	.2	.2	.6	1.3
Ilmenite	1.1	.9	.8	.5	.8	.8	.7	.7	.6	.1
Apatite	.5	.6	.4	.5	.6	.4	.3	.3	.4	.2
Calcite	---	.1	---	---	.5	.1	---	---	---	.1
Phenocrysts (volume percent)										
Plagioclase	27.7	17.2	12.2	8.6	25.6	8.6	15.0	16.0	21.0	5.2
Microlites	---	56.1	73.0	71.4	---	54.2	---	5.7	17.2	36.2
Olivine	6.1	---	---	---	---	---	---	---	---	---
Clinopyroxene	3.1	---	---	---	---	4.2	---	---	---	---
Orthopyroxene	t	---	t	---	---	2.4	---	---	---	---
Hornblende	.6	11.4	5.6	6.6	---	3.0	7.8	2.4	6.6	---
Biotite	---	2.2	3.0	1.6	8.6	.2	13.1	4.2	6.4	---
Quartz	---	---	---	.2	.6	---	---	---	---	.2
Opaques	4.6	10.1	6.0	9.4	3.2	5.8	6.8	2.8	4.2	8.8
Groundmass	57.7	3.0	---	2.2	62.0	21.6	57.3	65.2	44.6	42.6
Ox-mafics	---	---	---	---	---	---	---	---	---	7.0
VRF	---	---	---	---	---	---	---	3.6	---	---
TOTAL	99.8	100.0	99.8	100.0	100.0	100.0	100.0	99.9	100.0	100.0

Hornblende, from 0.25 to 1.0 mm in diameter, occurs alone or in clots with plagioclase. Brown-green pleochroism and cleavage at ~56° and ~124° are diagnostic of hornblende. Oxidation has reduced some crystals to skeletal, reddened outlines, and others show a thin (~0.10 mm), dark alteration rind. Birdseye extinction and dark-brown pleochroism are present in most booklets of biotite. In others, pleochroism is a deep red brown suggestive of oxybiotite. Biotite cut parallel to (001) is approximately 0.25 mm in diameter. Disequilibrium is indicated by resorption embayments and the possible exsolution of iron has formed magnetite euhedra. Cumulocrysts of plagioclase rarely enclose biotite, indicating that biotite grew later or nucleated separately.

Euhedral clinopyroxene is identified as augite based upon the moderate 2V (~45°-60°), octagonal cross section, and absence of pleochroism. Grains range in size from 0.10 mm to 0.20 mm and are solitary or occur in cumulophyric clots with plagioclase. The euhedral shape of most opaques indicates magnetite. However, the splintery form and reddened margins on others suggest oxide pseudomorphs after hornblende or biotite. The crystal-rich groundmass is weakly granophyric, pilotaxitic with plagioclase microlites, and is spotted with magnetite euhedra (~0.01 mm).

Quartz-bearing rhyodacite

The quartz-bearing rhyodacite is gray to reddish gray and porphyritic with plagioclase and varying amounts of biotite and hornblende. Thickness of the flow appears to be less than 50 m. Use of quartz xenocrysts as a unique flow marker is questionable, but the stratigraphic position and presence of quartz help define this subtype.

The high silica content of all the rhyodacites (table 2), between 65.9 and 69.8 percent, implies the presence of quartz, either phenocrystic or occult in the groundmass (Nockolds and others, 1978). Quartz in a volcanic rock has two likely sources--crystallization from a silica-saturated melt or xenocrysts from quartz-bearing rocks from below the volcano. Criteria for differentiating volcanic from xenocrystic quartz are outlined in Folk (1974, p. 70).

Phenocrysts of plagioclase and hornblende are bound in a glassy to granophyric matrix. The groundmass is pilotaxitic with plagioclase microlites and shows devitrification spherulites (<0.10 mm) and granophyric mosaic. Phenocrysts of plagioclase (An_{38-44}) range in size from 0.25 mm to 1.0 mm, while cumulocrysts are 1.0 mm with rare aggregates up to 4.0 mm. Pericline, albite, and Carlsbad twins are present in both the lath and tablet phases. Oscillatory, reverse, and normal zoning are also present. Resorption features indicating disequilibrium, perhaps incurred during ascent of the magma, are present as dusty, glass-shot rims around the plagioclase. Resorption effects are generally localized at the grain margin.

The most abundant mafic mineral is hornblende, which occurs in monomineralic clots up to 2.0 mm or as free crystals 0.50 mm in diameter. Both types have thin, oxidized margins, generally less than 0.10 mm, and display typical amphibole cleavage and pleochroism. Pleochroic biotite is present with birdseye extinction and iron oxide accentuating the 0.45 mm grains is present. The groundmass is flecked with euhedral (0.10 mm) opaques and a birefringent mineral suggestive of clinopyroxene, but too small for flat-stage determination. Opaques are embayed magnetite euhedra ranging in size from 0.25 to 0.50 mm.

Quartz is less than one percent of the mode, and its small size (<0.50 mm) makes a morphological determination of its origin uncertain. Xenocrystic origin of the quartz is suggested because of the absence of embayments and bipyramidal outline typical of volcanic quartz. However, the silica content of the rock, 68 to 69 percent, is near the upper end of the chemical field for rhyodacites, weakly implying the cognate origin of the quartz.

Two-pyroxene rhyodacite

A distinct two-pyroxene rhyodacite crops out at one locality southeast of Viola's Peak. Approximately 8 m of brecciated, basal vitrophyre remains as the only exposure of this petrographically distinct flow. If a minimum of 20 m is allowed for the carapace and interior of this flow, then a total of approximately 30 m could be added to the composite section.

This autoclastic, monolithologic rock displays elliptical and oriented fragments of vitrophyre in a devitrified matrix, each having plagioclase phenocrysts of the same composition. No welding or compression of the fragments has taken place, but the striking megascopic feature is its fragmented, oriented appearance. The clasts are not readily apparent in thin section unless devitrification features are present in the interfragment matrix.

Abundant clinopyroxene, 4 percent, and orthopyroxene are present. Orthopyroxene (hypersthene) comprises 2 percent of the mode, while in other flows it is present in trace amounts. The negative optic sign, distinctive cleavage, and faint pleochroism indicate hypersthene. Augite euhedra are generally larger, 0.45 mm and have a positive sign as well as a moderate 2V ($\sim 60^{\circ}$). Clinopyroxene also occurs as euhedra (0.05 mm) in the groundmass and in cumulocrysts with plagioclase.

Thin section shows a seriate-porphyritic texture consisting of 0.10 mm microlites, 0.40 mm phenocrysts and clots from 0.75 mm to 2.0 mm. The phenocrysts, plagioclase, clinopyroxene, and quartz, are not abundant and contain numerous glass inclusions in their margins. Microlites of plagioclase are more abundant (54.2 percent) than phenocrysts (8.6 percent) and the anorthite content, An_{28-50}, is representative of the microlite assemblage. Both hornblende and sparse biotite are present. Amphibole is ghost-like in appearance with magnetite grains silhouetting the former hornblende. Pleochroism of the biotite is copper red, indicating oxybiotite.

Low-silica rhyolite

The low-silica rhyolite is crystal poor, pilotaxitic, and has sparse plagioclase, biotite, and hornblende. One sample from a small valley west of Viola's Peak shows a fine-grained, finely flow-foliated texture. The high silica content of this sample was suspected but not confirmed until later analysis (table 2, column 10).

This rhyolite overlies volcaniclastic rocks at Negro Ben Peak and is overlain by volcaniclastic rocks in the locality near Viola's Peak. Thickness is approximately 60 m, but the uncertain stratigraphic relations and different textures suggest the presence of several low-silica rhyolites.

Phenocrystic quartz is not present in the low-silica rhyolites, which have a SiO_2 content ranging from 70.2 to 73.2 percent. Xenocrystic quartz, present in only one sample, is less than 1 percent of the mode, whereas normative quartz is present for all samples.

Plagioclase occurs as phenocrysts (1 mm) and as crystal clots with biotite (1-2 mm). The anorthite content of the twinned crystals is low and ranges from An_{26} to An_{46}. Carlsbad, albite, and pericline twins are present as well as equant tablets which are normally zoned. Disequilibrium is indicated by a margin of corrosion pits or the entire crystal is corroded.

Biotite and hornblende are the most common mafic minerals, with clinopyroxene limited to polycrystalline aggregates. Biotite exhibits dark-brown pleochroism, ripple-like birdseye extinction, and a faint oxidation rind. Both splintery microlites and 0.5 mm booklets are present. Hornblende euhedra are generally 0.4 mm in diameter and show distinctive cleavage and green-brown pleochroism. Biotite and hornblende have been oxidized, developing an intense pleochroism and opaque iron oxides. The biotite crystals are alined. Dark-red hematite masks the extinction pattern of biotite. Some of the needle-like, oxidized mafics could have been hornblende. Magnetite is present as an exsolution product of the mafics or as 0.10 mm subhedral to anhedral grains in the groundmass. The groundmass may be isotropic or nonisotropic but always shows a fluidal, pilotaxitic structure that has abundant biotite and plagioclase microlites. Devitrification mosaic is sparsely present.

Basalt of Malpais Mesa

A 6- to 8-m-thick basalt flow, informally named here as the basalt of Malpais Mesa, is exposed in the eastern part of the study area. Its relation to the lavas of McLendon volcano is uncertain, but it is structurally significant as the flow has not been affected by basin-and-range faulting. The basalt caps an unfaulted 100 m section of late Tertiary basin-filling gravels and sands; this contact is reddened and oxidized and, in turn, the basalt is locally overlain by a 1 to 2 m section of algae-bearing micritic limestone.

The flow was not thick enough or viscous enough to form basaltic structures such as entablature and colonnade, but small-scale features such as angular millimeter-sized vugs and pipe vesicles are commonly found. The vent for this flow is uncertain as the limited outcrop area of this flow shows few directional features. Silica content of the basalt is 49.9 percent (table 3); an age of 11.8±1.1 m.y. is based on a single whole rock K-Ar age (Neil Suneson, written commun., 1978).

The basalt of Malpais Mesa is an olivine basalt, diktytaxitic, dark gray to black, and lacks solitary plagioclase phenocrysts. In thin section the rock has a subophitic texture of clinopyroxene with plagioclase (An_{35-55}), which is the primary framework mineral. Twinned plagioclase laths, up to 3.0 mm, are abundant while normally zoned tablets are less common. Minor resorption textures are present but the overall appearance of the plagioclase indicates equilibrium.

Olivine is present as subhedral phenocrysts (~2.0 mm) and may encase laths of plagioclase. A high Mg content (2V~90) is indicated and is compatible with the presence of calcic to intermediate plagioclase. Iddingsite is ubiquitous and partially or thoroughly replaces olivine. Jackets of olivine rim the iddingsite, indicating continued crystallization of olivine after the alteration process stopped. It is very likely that this late-stage olivine is more iron rich and represents the composition of the groundmass olivine. The clinopyroxene is augite ($2V\sim60^{o}$), 0.1 to 0.2 mm in diameter, and has a subophitic texture. Partially resorbed magnetite and splintery ilmenite are present in the dark, iron-rich groundmass.

Table 3.--Analyses of basalt of Malpais Mesa, Yavapai County, Ariz.

[Method as described under "single solution" in U.S. Geological Survey Bulletin 1401; analysts, H. R. Smith and J. E. Reid]

Basalt of Malpais Mesa					
Field No.-- 100-77 Lab. No.--- W-200273 subophitic					
Major oxides (weight percent), recalculated without H_2O and CO_2		Norms (weight percent)		Phenocrysts (volume percent)	
SiO_2--------	49.9	Quartz----------	---	Plagioclase-----	47.6
Al_2O_3-------	15.2	Corundum--------	---	Olivine---------	22.8
Fe_2O_3-------	3.4	Orthoclase------	6.5	Clinopyroxene---	13.4
FeO---------	8.4	Albite----------	23.9	Opaques---------	5.2
MgO---------	7.4	Anorthite-------	25.6	Groundmass------	11.0
CaO---------	10.1	Di-Wollastonite-	9.4	TOTAL	100.0
Na_2O--------	2.8	Di-Enstatite----	5.6		
K_2O---------	1.1	Di-Ferrosilite--	3.3		
TiO_2--------	1.3	Hy-Enstatite----	6.7		
P_2O_5--------	.2	Hy-Ferrosilite--	4.0		
MnO---------	.2	Ol-Fosterite----	4.2		
TOTAL	100.0	Ol-Fayalite-----	2.7		
H_2O+ -------	.7	Magnetite-------	5.0		
H_2O- -------	.3	Hematite--------	---		
CO_2---------	.1	Ilmenite--------	---		
		Apatite---------	0.4		
		Calcite---------	.3		

ROCK CLASSIFICATION AND MAJOR ELEMENT CHEMISTRY

Analyses of lavas of McLendon volcano are used to classify the rocks and compare them with similar data from nearby volcanic areas. The regional patterns are then compared with characteristic calc-alkaline, subduction-related volcanic rocks. Data are also plotted for the basalt of Malpais Mesa, and an ash-flow tuff that crops out along the east flank of the Harcuvar Mountains that is interpreted as related to McLendon volcano.

Rock classification is based on ratios of oxide abundance (Church, 1975). This method was chosen for its simplicity and because it requires minimum data manipulation (fig. 5). Bold letters are positioned at the averages for the rock types established by Daly (1933, cited in Church, 1975), and the dashed field outlines include the common ratios found for basalt, andesite, dacite, and rhyolite by Washington (1917, cited in Church, 1975).

Harker plots demonstrate variation in weight percent of oxides with increasing silica content (fig. 6). A smooth, linear plot suggests that the rocks evolved from a common source in a closed system. Plots showing the least scatter are Al_2O_3, $FeTO_3$, CaO, K_2O, and MnO against SiO_2. On the diagrams for TiO_2 and P_2O_5 against SiO_2, two points do not plot especially close to the trend of the other analyses. Excess P_2O_5 suggests secondary apatite. This alteration is not confirmed in thin section, and, if present, has not affected the plots for the other oxides, especially alteration-sensitive CaO, Na_2O, and K_2O. The increase in TiO_2 is approximately 0.3 weight percent and approximately 0.4 weight percent for P_2O_5. The insensitivity of P_2O_5 and TiO_2 to alteration (Gottfried and others, 1977) and the concordance of these points on the other diagrams suggest that the apparently excess amounts are typical of this flow and do not necessarily indicate alteration.

A plot of water-free CaO, $Na_2O + K_2O$ against SiO_2 indicates that the lavas of McLendon volcano are calc-alkaline (fig. 7). The high-alumina values of the McLendon rocks (~16 percent), porphyritic texture, presence of plagioclase, clinopyroxene, orthopyroxene, hornblende, and biotite, and position on the alkali-lime index at ~60 percent SiO_2 within the calc-alkaline field of 56 to 61 percent SiO_2 demonstrate the calc-alkaline character of these rocks.

Both oceanic island arcs, typically lower in K_2O, and continental arcs are included in the calc-alkaline association, even though details of subduction and tectonism are different (Green and Ringwood, 1968). On figure 8 the AFM diagram shows that the analyses for McLendon volcanic rocks fall within the field established by Ringwood (1975, p. 237) for calc-alkaline rocks as typified by the Aleutian, Cascade, and New Zealand trend. Published analyses for other parts of the transition zone--the Peach Springs Tuff (Fuis, 1974), averages for the Mogollon-Datil volcanic field (Ratté and Grotbo, 1979), the Vulture Mountains (Rehrig and others, 1980), the Superior volcanic field (Sheridan and others, 1970), and the Oatman district (Thorson, 1971) also plot within the calc-alkaline field. The similarity of all these calc-alkaline volcanic suites suggests formation of these magmas in a similar tectonic environment.

The high alumina, from 14.5 to 17.5 percent, minimal iron enrichment, K_2O/Na_2O ~.6 at 40-60 percent SiO_2, and the mineral assemblage of biotite, hornblende, clinopyroxene, and orthopyroxene suggest that depth to the subducted slab that generated the McLendon lavas was from 120 to 220 km (Keith, 1978). This is shallower than the predicted depth of 290 km for the Oatman district (~130 km to the northwest of McLendon volcano) as interpreted by Lipman and others (1971) based on K_2O-depth plots.

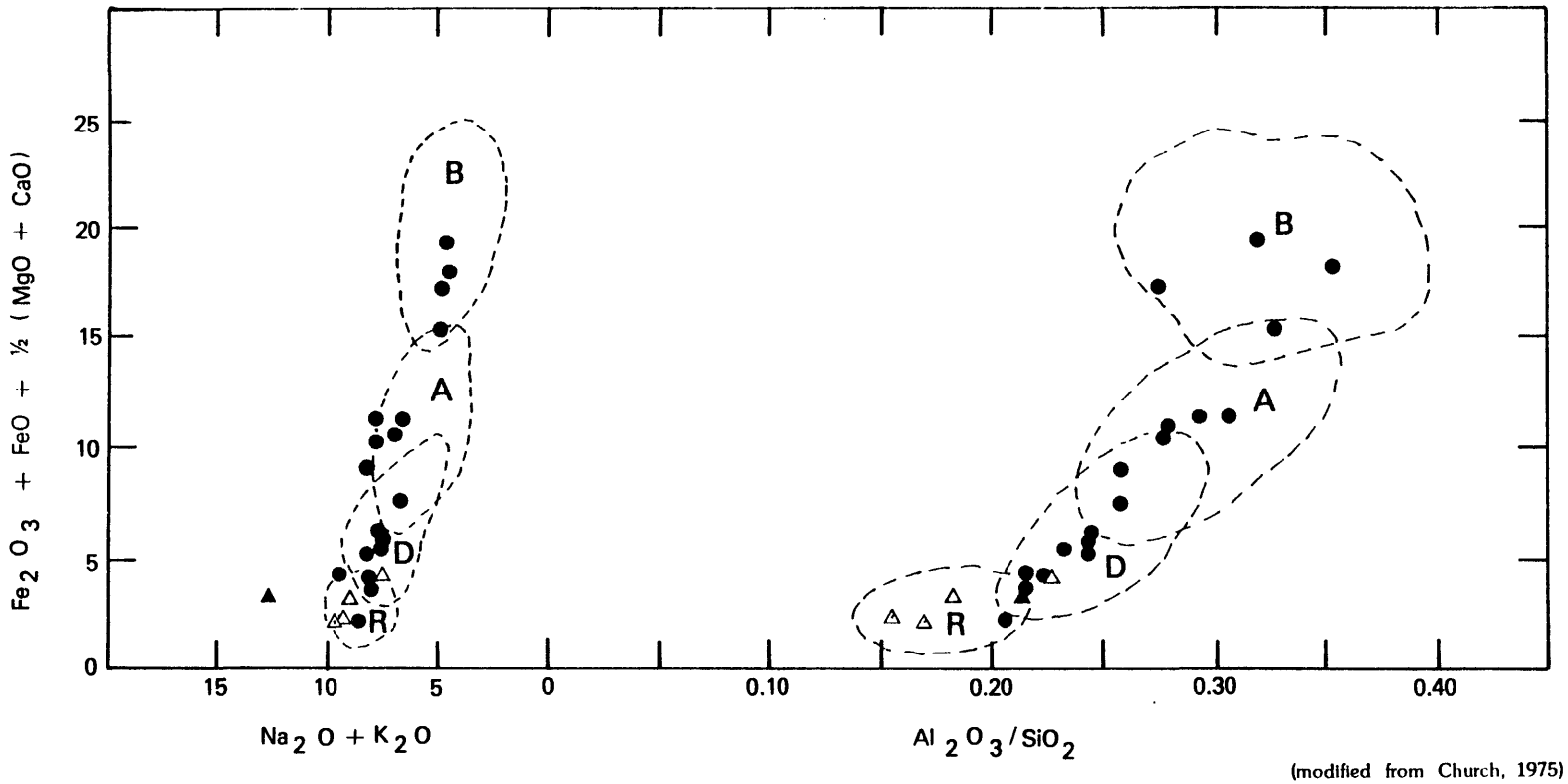

Figure 5.--Church classification for analyses of volcanic rocks from ●- McLendon volcano; ▲, △* ash-flow tuff of Harcuvar Mountains (table 5). Dashed outline shows fields for common volcanic rocks (B - basalt, A - andesite, D - dacite, R - rhyolite) (Washington, 1917, cited in Church, 1975). [Analysis as described under "single solution" in U.S. Geological Survey Bulletin 1401; analysts: H. R. Smith and J. E. Reid; * analysis by X-ray spectroscopy; analysts: J. S. Wahlberg, J. E. Taggart, J. W. Baker]

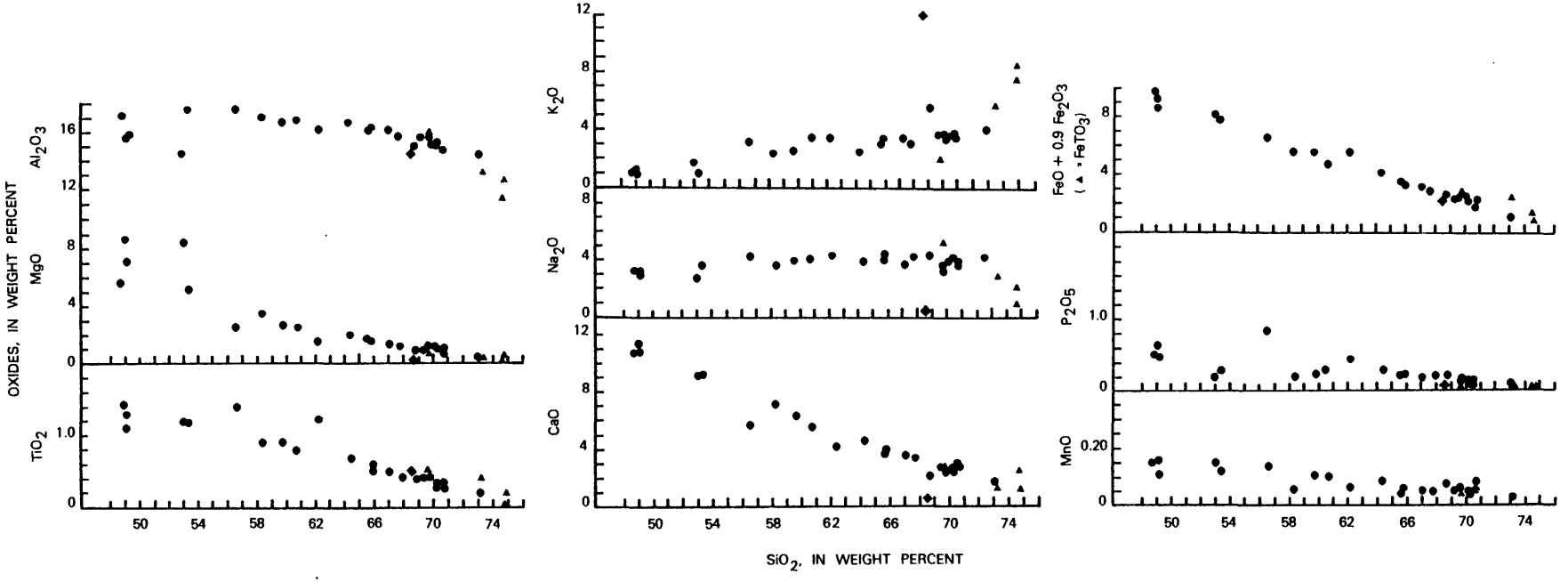

Figure 6.--Harker variation diagrams for analyses of volcanic rocks from: ●- McLendon volcano; ◆, ▲* ash-flow tuff of Harcuvar Mountains; [Analysis as described under "single solution" in U.S. Geological Survey Bulletin 1401; analysts: H. R. Smith and J. E. Reid; * analysis by X-ray spectroscopy; analysts: J. S. Wahlberg, J. E. Taggart, J. W. Baker; $FeTO_3$ indicates total iron reported as Fe_2O_3]

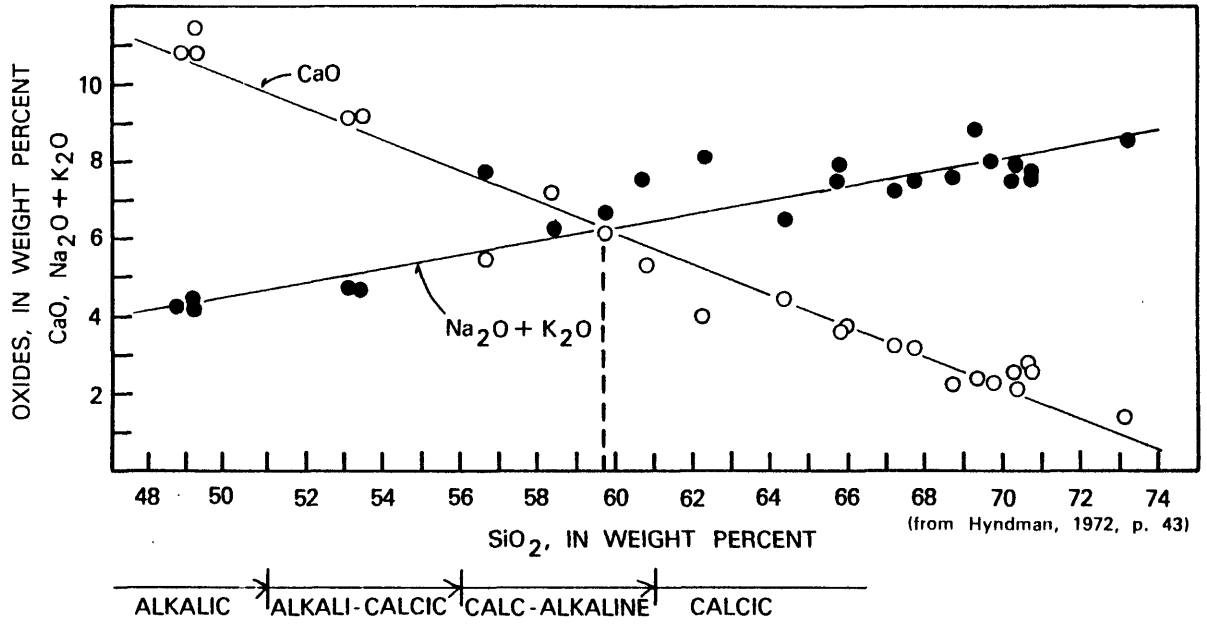

Figure 7.--Alkali-lime index for analyses of volcanic rocks from McLendon volcano. (Line placement is by inspection.)

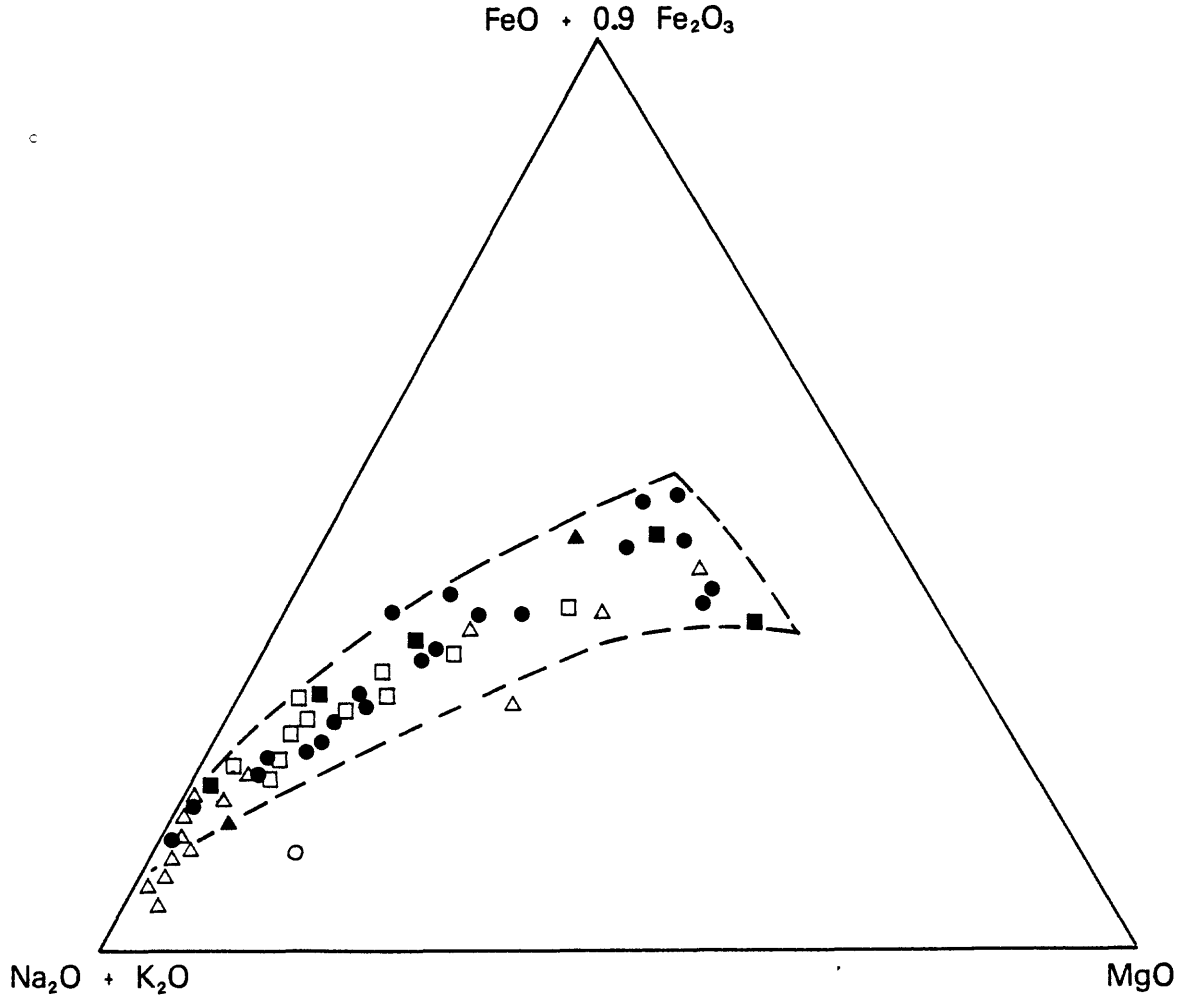

Figure 8.--AFM diagram for analyses of lavas of the transition zone. Dashed line encloses the calc-alkaline trend of the Aleutians, Cascades, and New Zealand (Ringwood, 1975).

● - McLendon volcano	This report
○ - Peach Springs Tuff	Fuis, 1974
▲ - Mogollon-Datil volcanic field (averages)	Ratté and Grotbo, 1979
△ - Vulture Mountains	Rehrig and others, 1980
■ - Superior volcanic field	Sheridan and others, 1970
□ - Oatman district	Thorson, 1971

Basin-and-Range silicic volcanic rocks with K_2O content around 8 percent have been called trachytic or ultrapotassic (Rehrig and others, 1981, cited in Keith and others, 1981, p. 69). The chemistry of these rocks does not represent melt compositions.

The terminology is equally problematic for rocks that have less than 8 percent K_2O, as shown on figures 9 and 10 in which the same data for McLendon rocks are plotted on two different diagrams. Figure 9 shows the analyses to be within the range for average rocks, but close to the K-rich border, and figure 10 shows that the same rocks are K-rich and out of the calc-alkaline field.

The McLendon rocks are typical of continental margin calc-alkaline rocks based upon the mean $(FeO + Fe_2O_3)/MgO$ value of 2.8 and the mean K_2O/Na_2O value of 1.0 which is compared with the predicted, respective values of >2 and 0.60-1.10 (Jakes and White, 1972).

BASIN-AND-RANGE FAULTING

Description of faults

Three patterns of faulting are present at McLendon volcano, with each representing a different process. Most apparent are the regional northwest-trending basin and range faults that are complemented by a like-trending group of joints. Maximum displacement is 50 m, faults are steep, 60° to nearly vertical, and blocks are dropped down to the southwest. Some of these northwest-trending faults are cut off by local, northeast-trending faults. A local group of radial fractures southwest of the erosional wall of McLendon volcano may be related to late intrusive or resurgent activity within the volcano.

Faulting is most evident north of Tres Alamos (fig. 3) where portions of the volcaniclastic section are tilted against the younger rhyodacite. The fault plane is marked by slickensides, and a gouge zone ~20 cm in thickness. At some locations, offset is indicated where the dip of the finer grained volcaniclastic rocks projects into the juxtaposed, downthrown block of rhyodacite.

Mapping faults and measuring the displacement within parts of the volcanic section are difficult, especially within thick rhyodacite flows of similar mineralogy. Rare fault breccias and subtle facies relationships help to determine stratigraphic offset. The lower portion of the rhyodacite flow is generally "poker-chip" in appearance and contrasts with the massive, contorted flow interior. Basal vitrophyre or a glassy breccia generally marks the base of a flow--but this presents little contrast to the sometimes glassy, brecciated carapace of an underlying flow. Thin interbeds of volcaniclastic rocks can also be used as marker units, but even their use is not dependable due to their sporadic appearance within the section.

Also present in the map area is a minor pattern of joints and fractures. These features are most apparent on the aerial photographs and are noted as thin lines on the geologic map near Viola's Peak (fig. 3). These fractures seem related to basin-and-range faults because of their consistent northwest trend.

An arcuate fracture pattern southwest of Viola's Peak is interrupted by several east-northeast-trending radial fractures, all contrary to the strong northwest pattern of the map area. The radial fractures suggest diapiric movement from below, much like a salt plug (Landes, 1959, p. 344), and could have resulted from tension created by an aborted resurgent episode. This arcuate pattern is only evident near the inferred erosional wall of McLendon volcano.

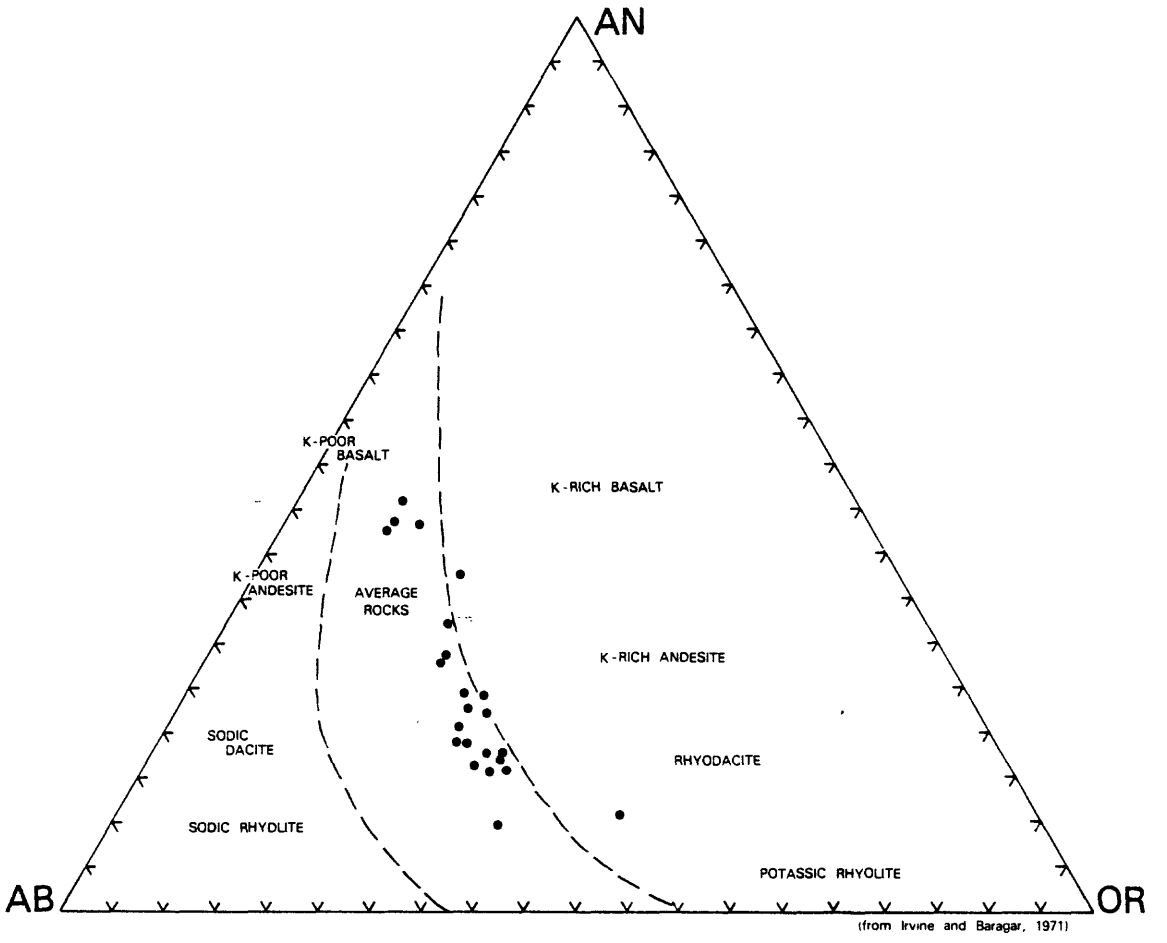

Figure 9.--Plagioclase ternary diagram, based on normative minerals, used to distinguish potassium-poor, -average, and -rich variants. Analyses are of McLendon lavas only.

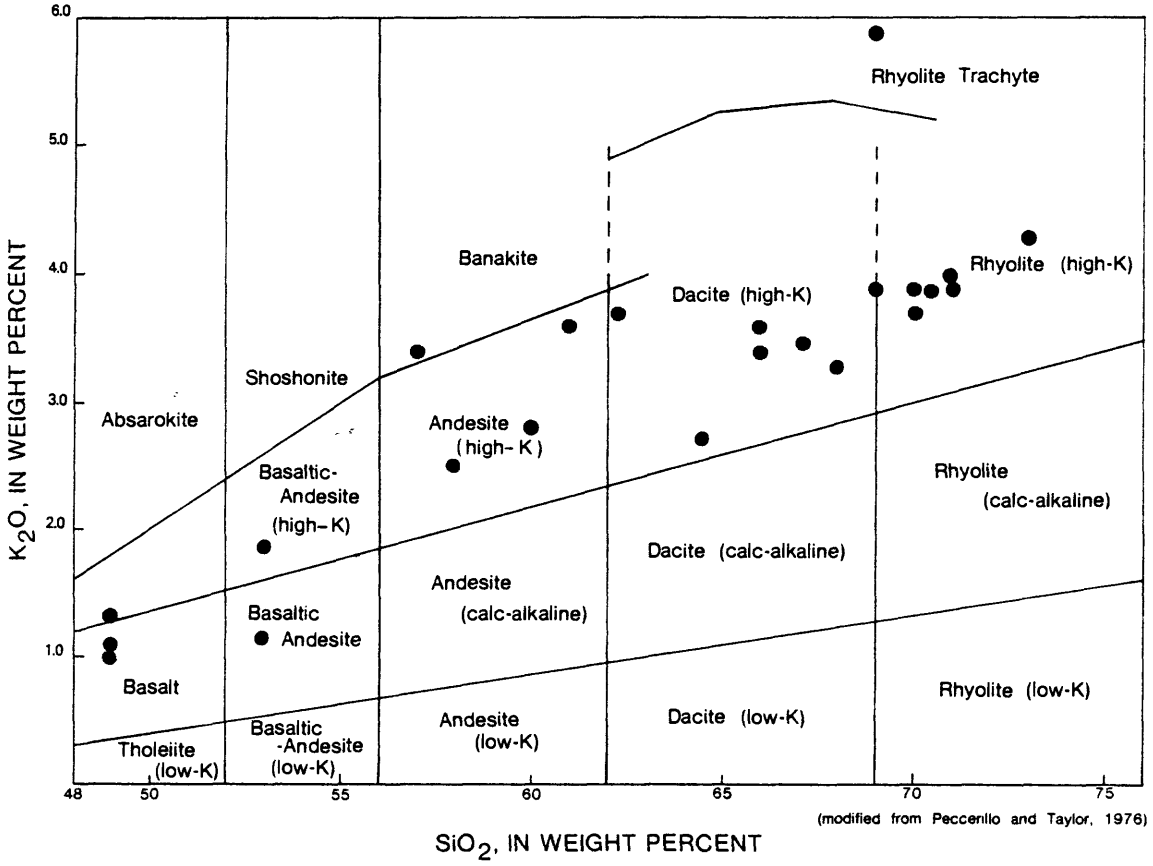

Figure 10.--K_2O against SiO_2 plot showing analyses of McLendon volcanic rocks in the high-K field of Peccerillo and Taylor (1976).

Mechanism and timing

Underthrusting of the Farallon plate during mid-Tertiary time is considered to be the mechanism that triggered eruption of andesitic to rhyolitic rocks in southwestern North America (McKee, 1971). Collision and demise(?) of the oceanic ridge that bounded the Farallon plate, about 19 million years ago, terminated subduction-related tectonics and marked the onset of Basin-and-Range faulting and basaltic volcanism (McKee, 1971).

Onset of subduction-related volcanism varies within the Basin and Range and along the transition zone. Different researchers present the following dates based on field mapping and isotopic ages of the volcanic rocks: prior to 26 m.y. and perhaps as early as 32 m.y. in the Chocolate Mountains of California (Crowe, 1978); prior to 30 m.y. in northern Arizona (Hamblin and Best, 1975); after 40 m.y. but prior to 20 m.y. within the Great Basin (McKee and others, 1970); and prior to 26 m.y. in the Vulture Mountains of southwestern Arizona (Rehrig and others, 1980).

Eruption of basalt through high-angle pull-apart structures marked the height of early basin-and-range tectonism. These undeformed flows are interlayered with similarly undeformed lacustrine and fluvial sediments and are, in turn, imposed on tilted, older strata (Shafiqullah and others, 1980). Dates for the onset of basaltic volcanism are: 13 m.y. in the Chocolate Mountains of California (Crowe, 1978); from 14.8 m.y. to 10 m.y. in north-central Arizona (McKee and Anderson, 1971); from 16 m.y. to 14 m.y. in the Vulture Mountains (Rehrig and others, 1980), and at 17.8 m.y. in the Aquarius Mountains of Arizona (Young and Brennan, 1974).

At McLendon volcano the subduction-related, calc-alkaline sequence is represented by the basalts, andesites, and rhyodacites of the volcano itself. Within this area of the transition zone, basin-and-range faulting occurred during or shortly after eruption of the 25-m.y.-old McLendon lavas. The olivine basalt preserved at Malpais Mesa is unfaulted within the limits of the study area and demonstrates the end of basin-and-range faulting in this area by 12 m.y. ago. However, mapping of correlative basalts outside of the study area might show effects of basin-and-range faulting, and the age of 12 m.y. in this part of the transition zone should be considered tentative. A bracket for basin-and-range faulting is established between its onset sometime after 25 m.y. ago and its termination approximately 12 m.y. ago.

EVIDENCE FOR CALDERA COLLAPSE

Approximately one-third of McLendon volcano remains as an arcuate outcrop--the north and east flanks of a composite volcano. Erosion has removed as much as 490 m of volcanic and volcaniclastic rock near Negro Ben Peak where basal vitrophyre and volcaniclastics, composed of metamorphic and lithic fragments, are perched on Precambrian rocks at 3,250 ft (990 m). An outcrop of metamorphic-lithic volcaniclastic rock is found at the level of the Santa Maria River at 1,640 ft (500 m), and suggests, in the apparent absence of 500 m faults, that a large portion of the stratigraphic section in the area of Negro Ben Peak has been removed by erosion.

In accounting for the absent southwest part of McLendon volcano, erosion is partially responsible, but the evidence presented below indicates caldera collapse as a possible explanation for the missing portion.

Gravity low

A circular, -25 mgal gravity low (Wynn and Otton, 1978) is centered southwest of the study area (lat. 34°15′ N., long. 113°15′ W.) (fig. 11). A

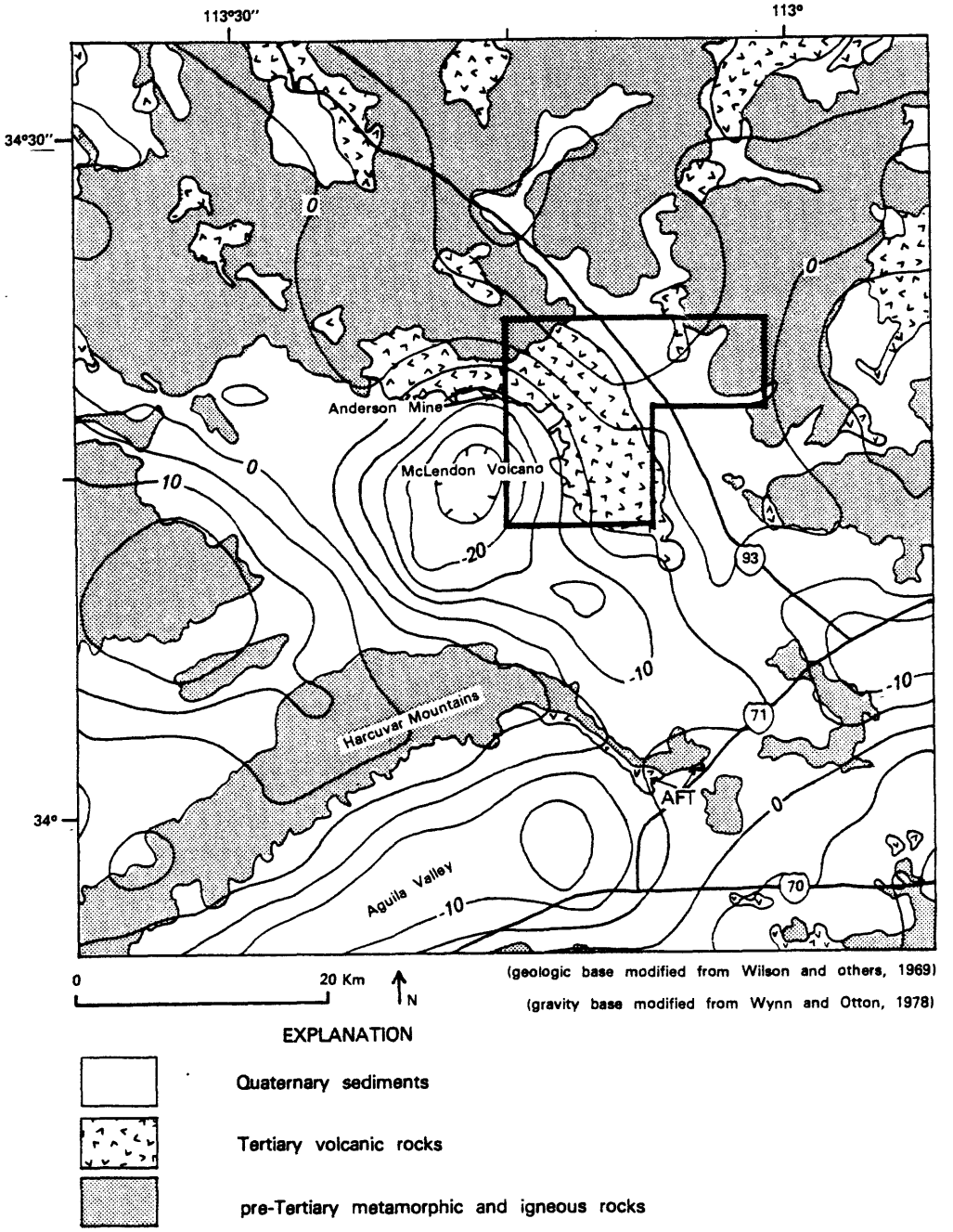

Figure 11.--Combined generalized geology and residual gravity map of McLendon volcano and vicinity. Study area is within heavy black line, contour interval is 5 mgal, and AFT indicates outcrops of ash-flow tuff of Harcuvar Mountains.

volcanic origin is proposed here for the McLendon low after consideration of the geologic and geophysical evidence. The circular shape and -25 mgal intensity of the McLendon low contrast with the northeast-elongate, -15 mgal Aguila Valley low to the south. Both are sediment-filled basins; one, Aguila Valley, is a product of sediment accumulation in a Basin-and-Range graben and the other, McLendon, is the result of low-density sediment accumulation in a collapsed(?) volcanic structure--or the expression of a shallow diapir.

The gravity signature of a volcano is an expression of the density contrast between the rocks of the region. Volcanoes associated with mafic lavas and intrusive basalts, such as Mauna Loa and Kilauea, show gravity highs of +100 mgals and +60 mgals, respectively (Kinoshita, 1963, cited in Williams and McBirney, 1979, p. 224). Gravity anomalies over silicic centers are generally negative owing to the abundance of explosive debris or the underlying low-density pluton such as at Long Valley, Calif. (-40 mgal) (Kane and others, 1976). The postulated Superior volcanic field near Phoenix, Ariz. (lat. 33°25′ N., long. 111°22′ W.) is the closest described silicic center. Its gravity signature is poorly defined and the Luke Salt gravity low (Eaton and others, 1972), to the northwest, is a more conspicuous low (fig. 12).

In the San Juan volcanic province of Colorado, many of the silicic cauldrons do not have the anticipated gravity low stacked over the collapse structure (Plouff and Pakiser, 1972). This is due to the absence of sufficient density contrast with the surrounding rocks, because the calderas have collapsed into rock of similar composition and density, and because the underlying intrusion is larger than the caldera. The density contrast of the rock types exposed within the volcanic field can mask, as in the San Juans, or accentuate the intensity of the feature (Williams and McBirney, 1979, p. 233).

The rocks within the study area are Precambrian granites and metamorphic rocks with a bulk density of 2.6 to 2.7 g/cm^3, mafic to silicic volcanic rocks with an average density of 2.3 g/cm^3, and moderately indurated mid-Tertiary tuffaceous lake sediments with a density of 1.8 to 2.0 g/cm^3 (McKeown, F. A., personal commun., 1978). The difference in bulk density of these rock types, as well as the possibility of an underlying diapir, provide possible explanations for the McLendon gravity low.

Concentric strike pattern

The arcuate, concave to the southwest, outcrop pattern of the volcanic rocks within the study area, and the north- to northeast-radiating dip pattern of flow foliation imply that a 20-km-diameter volcanic center was located astride the -25 mgal gravity low (fig. 11). This is about equal in size to the nearby Superior cauldron (20 km in diameter) and related calderas averaging 8 to 10 km in diameter within the Superior volcanic field (Sheridan and others, 1970).

For comparison the diameters of several other calderas:

Aso	Kyushu Island, Japan	20 km
La Garita	San Juan Mtns., Colo., U.S.A.	45 km
Valles	Jemez Mtns., N. Mex., U.S.A.	21 km

and stratovolcanoes are listed:

Mt. Rainier	Washington, U.S.A.	16 km
Mt. Hood	Oregon, U.S.A.	18 km
Mt. Mayon	Philippines	11 km

(MacDonald, 1972, p. 284, 303).

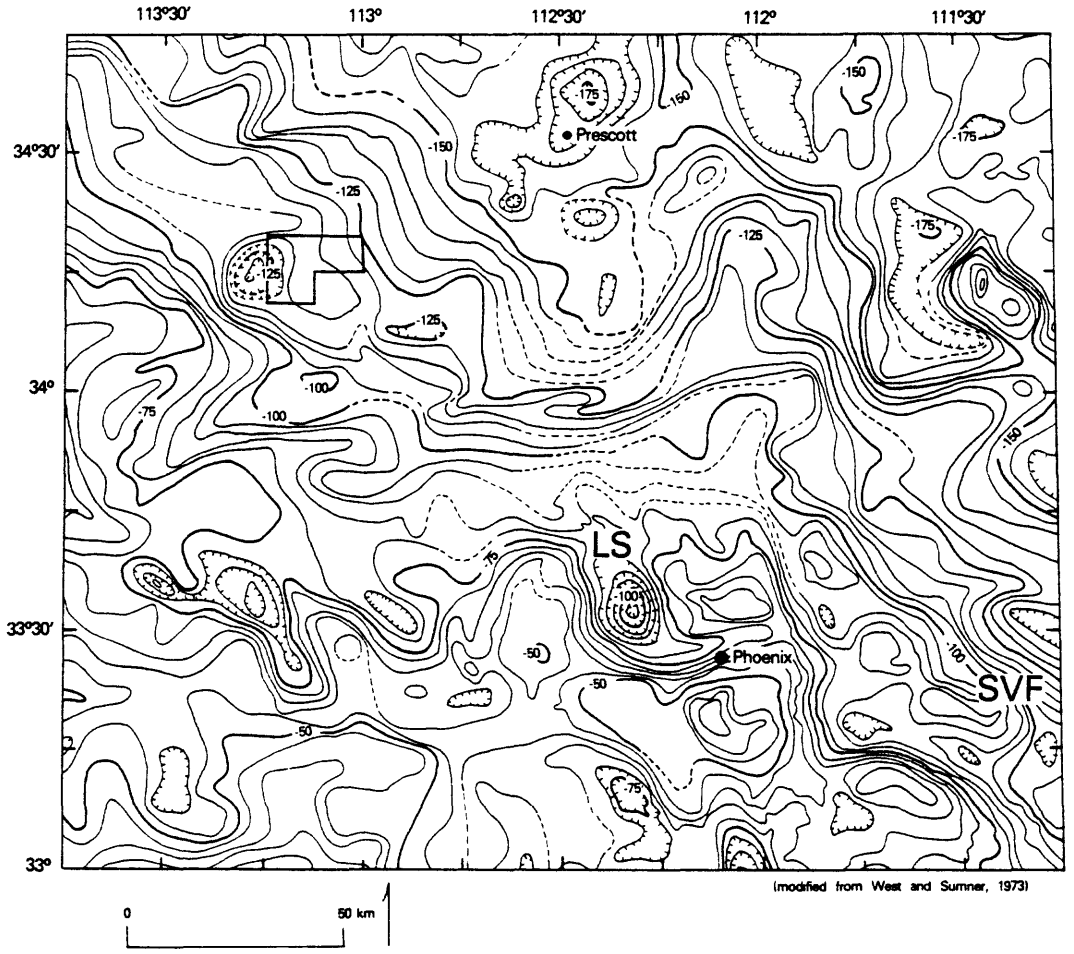

Figure 12.--Portion of Bouguer gravity map of Arizona with study area outlined (contour interval is 5 mgals). Note generalized location of Superior volcanic field (SVF) near lat. 33°25′, long. 111°22′ and Luke Salt low (LS) northwest of Phoenix.

Volcanic facies

The exposed rocks on the northeast flank of McLendon volcano comprise thick lavas intertongued with lahars, that contain blocks up to 5 m in diameter, and reworked volcaniclastic debris. Applying the volcanic facies concept of Williams and McBirney (1979, p. 313) such rocks would be found no farther than 15 km from the vent. Location of the vent fits with the geometric reconstruction of the center of the volcano over the gravity low located 12 km southwest of the study area.

Ash-flow tuffs and potassium metasomatism

Ash-flow tuff that may have been erupted from the McLendon volcano crops out along the eastern flank of the the Harcuvar Mountains (fig. 11). From base to top, the ash-flow tuff is a simple cooling unit consisting of a welded biotite-bearing vitrophyre, a biotite-bearing, devitrified zone with flattened pumice (1.0 cm x 1.0 mm), a spherulitic (2.0-3.0 cm in diameter) zone, a gray, biotite-bearing welded zone, and a fine-grained perthite-bearing ash-flow tuff. Eutaxitic structures are common and are steeply dipping, ~60-70° to the southwest. The steep dip indicates that the tuffs are not in their original position.

The ash-flow tuff found along the flank of the Harcuvar Mountains has been sampled, but not mapped in detail. Analyses for the tuff (table 4) are compared (fig. 5) with analyses for McLendon volcanic rocks of a similar SiO_2 content (table 2). Most striking in this comparison is the range (2.3-12.0 percent) and median (7.3 percent) of K_2O content for the tuff when compared to the range (3.3-5.9 percent) and median (4.1 percent) K_2O content for the rocks of McLendon volcano. These potassium metasomatized ash-flow tuffs, especially sample E-191D, have mistakenly been called high-potassium trachytes (Scarborough and Wilt, 1979, cited in Keith and others, 1981, p. 78). Abundant secondary potassium is revealed by staining; however, the unstained section shows no evidence of alteration. The age of the tuff is 23.9±0.9 m.y. based on a K-Ar determination on biotite (R. F. Marvin and others, written commun., 1982).

The trend of analytical data for the ash-flow tuff is very similar to the data for the volcano itself--with the exception of the alkalies (figs. 5 and 6). This chemical similarity and age relations suggest a genetic relationship between McLendon volcano and the ash-flow tuff; however, the case is arguable as erosion and basin-and-range faulting have removed other portions of the tuff that may have shown continuity with McLendon volcano.

The potassium metasomatism that has altered the ash-flow rocks could be due to thermal effects brought on by the mechanisms involved in listric faulting (Rehrig and others, 1981, cited in Keith and others, 1981, p. 73). Both K and Na metasomatism have altered these rocks, and the steep dips indicate the tortured response of this area to the mechanisms of listric faulting. It is significant that the effects of metasomatism and listric faulting diminish to the north of the Harcuvar area toward McLendon volcano and north of the Vulture Mountains toward Wickenburg. Both origin of the ash-flow tuff and subsequent metasomatism are in need of further investigation; however, McLendon volcano is the closest known volcanic center and is a likely source for the ash-flow tuff.

Trace element patterns

Certain trace elements concentrate during differentiation and should be obvious in the late-formed minerals (Smith and Bailey, 1966). Their studies

Table 4.--Analyses of ash-flow tuff (AFT) cropping out along the east flank of the Harcuvar Mountains, Yavapai County, Ariz.

[*Analysis as described under "single solution" in U.S. Geological Survey Bulletin 1401, analyst: Z. A. Hamlin; all others by X-ray spectroscopy, analysts: J. S. Wahlberg, J. E. Taggart, J. W. Baker. nr: not reported; $FeTO_3$ indicates total iron reported as Fe_2O_3]

	Ash-flow tuffs				
Field No.-- Lab No.----	E-191B D-235899 biotite-bearing vitrophyre	E-191C D-235900 biotite-bearing devitrified AFT	E-191D W-205351* spherulite-bearing AFT	E-191E D-235901 upper biotite-bearing devitrified AFT	E-191F D-235902 perthite-bearing AFT
Major oxides (weight percent), recalculated without H_2O and CO_2					
SiO_2-------	70.0	73.3	68.6	74.7	74.8
Al_2O_3------	16.0	13.3	14.8	12.6	11.5
Fe_2O_3------	nr	nr	2.6	nr	nr
FeO--------	nr	nr	.1	nr	nr
$FeTO_3$------	2.9	2.6	nr	1.6	1.1
MgO--------	.8	.4	.3	.2	.5
CaO--------	2.4	1.1	.6	.9	2.3
Na_2O-------	5.0	2.9	.4	2.0	.9
K_2O--------	2.3	5.9	12.0	7.7	8.7
TiO_2-------	.4	.4	.5	.2	.1
P_2O_5-------	.1	.1	.1	.1	.1
MnO--------	.1	<.1	nr	<.1	<.1
TOTAL	100.0	100.0	100.0	100.0	100.0
H_2O+ ------	nr	nr	.7	nr	nr
H_2O- ------	nr	nr	.1	nr	nr
CO_2--------	nr	nr	---	nr	nr
LOI--------	6.1	0.9	nr	1.1	2.8

of the Bandelier Tuff eruptive sequence showed that Nb, Ta, U, Th, Cs, Rb, Li, Sn, Be, B, W, Mo, Cl, F, Pb, Zn, and Sm concentrate upwards within the system and would be enriched in cyclical or terminal magmatic events--particularly in ash-flow eruptions.

Accordingly, three samples of flow rock from the McLendon area and a sample of ash-flow tuff from the Harcuvar Mountains were analyzed for U, Th, and several other trace elements (tables 5, 6). Uranium content for the McLendon flow rocks is from 1.7 ppm to 3.2 ppm, and for the ash-flow tuff of the Harcuvar Mountains it is 10 ppm. It is unlikely that 10 ppm is the original U content of the ash flow as some leaching and alteration losses must be considered. Thorium content of the ash-flow tuff is higher, 23.7 ppm, than the values for the lava flows, 7.0-13.1 ppm (table 5).

Other elements such as Ba, Sr, Eu, Ti, Cr, Co, Sc, Au, and Cu concentrate downward in the chamber and ash-flow eruptions would be depleted in these elements (Smith, 1979). Concentration of Sr as well as the Rb/Sr ratio should follow a predictable pattern with Sr decreasing and the Rb/Sr ratio increasing with differentiation. The mean Rb/Sr ratio of the McLendon suite is <0.1 for the basalts and andesites, 0.2 for the silicic rocks, and 3.6 for the ash-flow tuffs of the Harcuvar Mountains (table 6). Based upon the increasing mean Rb/Sr ratio, it is permissive that these rocks are genetically related to McLendon volcano. The alteration that has affected the ash-flow rock has probably clouded the reliability of the Rb/Sr ratios, and, unfortunately, unmetasomatized rock is not available at this time.

Uranium mineralization

Fossil hot springs were mapped by Otton (1977) during his study at the Anderson uranium property, 5 km west of the study area. The location of these ancient systems can be used to infer the caldera-marginal and resurgent fault systems (Hildreth and others, 1984), a likely pathway for uranium transport. Appreciable amounts of radioactive elements such as radon have been detected in hot springs in Italy by McDonald (1972), and uranium is reported from Mineral Mountains springs near Marysvale, Utah (Miller and others, 1979).

Field studies at the Anderson Mine by Sherbourne and others (1979) and Otton (1981) suggest that uranium mineralization is due to transport of leached uranium from nearby volcanic and granitic rocks and subsequent concentration in organic-rich lacustrine sediments as well as dewatering of local, volcanic-source, uranium-rich sediments.

Alternatively, the Anderson deposit could be volcanogenic in origin and comparable in volcanic setting to the Aurora prospect in the McDermitt caldera in Nevada (Roper and Wallace, 1981). The volcanic setting also suggests that the Anderson lake sediments are ponded, moat sediments within the outline of the McLendon caldera. If the Anderson deposit formed solely as a leachate from surrounding highlands, then the shape of the orebody might be somewhat similar in form to the classic Colorado Plateau roll-front deposits. However, the Anderson ore zones are tabular and stacked (Otton, 1981) as are the Aurora ore zones.

Based upon paleocurrent directions, Otton (1981) suggested that the ranges south and north of the Anderson mine were the likely source terrane for the uranium. The volcanic rocks found in these ranges can be eliminated as likely sources of uranium based on Th/U ratios.

The Th/U ratio of a nonhydrated, and therefore unleached, glassy tuff, the Belted Range Tuff, is 4.0. Correlative devitrified tuffs, based on field relations, major- and minor-element chemistry, especially Th, show a significantly higher Th/U ratio, averaging 16 (Rosholt and Noble, 1969).

Table 5.--Delayed neutron determinations of uranium and thorium for flow rocks of McLendon volcano and ash-flow tuff cropping out along the east flank of the Harcuvar Mountains, Yavapai County, Ariz.

[Analysts: H. T. Millard, R. B. Vaughan, M. F. Coughlin, M. N. Schneider, and W. R. Stang]

	Lavas of McLendon volcano			Ash-flow tuff of Harcuvar Mountains
Field No.---	162-78	204-79	210-79	E-191-D
Lab. No.-----	D-211402	D-211404	D-211405	D-211403
	Uranium and thorium (ppm)			
U----------	3.2	1.7	1.8	10.0
Th---------	13.1	9.2	7.0	23.7
Th/U-------	4.1	5.4	3.8	2.4

Table 6.--Selected trace-element content and ratios for lavas of McLendon volcano, ash-flow tuff of Harcuvar Mountains, and the basalt of Malpais Mesa

[Determinations from an activation analyzer Cd^{109} source; in ppm]

Field No.	Rb	Sr	Y	Zr	Nb	Rb:Sr	Y:Nb	Zr:Nb
			Basalt of Malpais Mesa					
100-77	10	271	18	104	2	<.4	9	52
			Ash-flow tuff of Harcuvar Mountains					
E-191F	326	149	24	153	28	2.2	.9	5.5
E-191E	257	33	19	261	24	7.8	.8	10.9
E-191D	326	47	21	389	26	6.9	.8	15
E-191C	178	167	24	347	25	1.1	1	13.9
E-191B	340	877	27	393	25	.4	1.1	15.7
			Silicic lavas of McLendon volcano					
174-78	181	440	10	157	4	.4	2.5	39.2
173-78	68	860	9	188	5	.1	1.8	37.6
169-78	108	624	7	146	6	.2	1.2	24.3
162-78	108	616	18	201	7	.2	2.5	28.7
156-78	94	906	15	144	6	.1	2.5	24
113-78	94	610	7	142	6	.2	1.2	23.6
			Mafic lavas of McLendon volcano					
212-79	20	1346	27	182	6	<.1	4.5	30.3
205-79	15	875	23	167	6	<.1	3.8	27.8
204-79	7	1472	26	188	12	<.1	2.2	15.6
203-79	79	940	20	187	5	.1	4	37.4
186-79	54	878	13	169	5	.1	2.6	33.8
138-77	43	599	32	333	15	.1	2.1	22.2

Belted Range tuff (Miocene), southern Nevada

		U ppm	Th ppm	Th/U
WPN-23	nonhydrated, glassy	5.5	21.8	4.0
WPN-109J	crystallized	1.3	19.5	15.0
BG-UN	devitrified	2.0	22.9	11.4
WPN-21B	devitrified	1.0	21.7	21.7

In comparison, the Th/U ratio of the ash flow of the Harcuvar Mountains, to the south, is 2.4 and the average Th/U ratio of the McLendon lavas, to the north, is 4.5 (table 5), both ratios being very close to 4.0, the ratio established by Rosholt and Noble (1969) for non-U depleted rocks and within the magmatic range of 2.5 to 5 of Rose and Bornhorst (1981). It seems unlikely that the ash flow of the Harcuvar Mountains or the lavas of McLendon volcano yielded sufficient uranium to generate the low grade Anderson orebody. The similarities between the Aurora prospect--clearly caldera-related--and the Anderson prospect indicate analogous structural settings and demand consideration of a similar volcanogenic origin of the uranium at Anderson Mine.

Other common geologic similarities between the volcanogenic Aurora prospect and the proposed volcanogenic Anderson prospect include bedding that is typically thin-laminar to varved, stacked orebodies, uranium that is not restricted to carbonaceous material, the occurrence of anomalous manganese and molybdenum, fossil hot springs, and the presence of carnotite and coffinite (Sherbourne and others, 1979; Otton, 1981; Roper and Wallace, 1981; Wallace and Roper, 1981).

It is proposed that caldera-marginal fault systems, and not the ash flow or lavas of the volcano itself, provided a pathway for late stage transport of uranium from a differentiated igneous source to the lake sediments.

SELECTED REFERENCES

Anderson, R. E., 1978, Chemistry of Tertiary volcanic rocks in the Eldorado Mountains, Clark County, Nevada, and comparisons with rocks from some nearby areas: U.S. Geological Survey Journal of Research, v. 6, p. 409-424.

Armstrong, R. L., Ekren, E. B., McKee, E. H., and Noble, D. C., 1969, Space-time relations of Cenozoic silicic volcanism in the Great Basin of the western United States: American Journal of Science, v. 267, p. 478-490.

Baker, Arthur, III, and Clayton, R. L., 1970, Massive sulfide deposits of the Bagdad District, Yavapai County, Arizona, in Ridge, J. D., ed., Ore deposits of the United States, 1933-1967 (Graton-Sales Volume): American Institute of Mining, Metallurgical, and Petroleum Engineers, v. 2, p. 1311-1327.

Best, M. G., and Brimhall, W. H., 1974, Late Cenozoic alkalic basaltic magmas in the western Colorado Plateaus and the Basin and Range Transition Zone, U.S.A., and their bearing on mantle dynamics: Geological Society of America Bulletin, v. 85, p. 1677-1690.

Blackwell, D. D., 1969, Heat flow determinations in the northwestern United States: Journal of Geophysical Research, v. 74, p. 992-1007.

Bohannon, R. G., and Anderson, R. E., 1978, Tertiary tectonic history of the eastern Basin and Range Province in the vicinity of Lake Mead in southern Nevada and western Arizona: Geological Society of America Abstracts with Programs, v. 10, p. 98.

Chapman, D. S., Furlong, K. P., Smith, R. B., and Wechsler, D. J., 1978, Geophysical characteristics of the Colorado Plateau and its transition to the basin and range province in Utah [abs.], in Plateau Uplift: Mode and Mechanism: Lunar and Planetary Institute Contributions 329, p. 10-12.

Christiansen, R. L., and Lipman, P. W., 1966, Emplacement and thermal history of a rhyolite flow near Fortymile Canyon, southern Nevada: Geological Society of America Bulletin, v. 77, p. 671-684.

_____1972, Late Cenozoic, pt. 2 of Cenozoic volcanism and plate-tectonic evolution of the Western United States: Royal Society of London Philosophical Transactions, v. 271, no. 1213, p. 249-284.

Christiansen, R. L., Lipman, P. W., Orkild, P. P., and Byers, F. M., 1965, Structure of the Timber Mountain caldera, southern Nevada, and its relation to basin-range structure: U.S. Geological Survey Professional Paper 525-B, p. B43-B48.

Church, B. N., 1975, Quantitative classification and chemical comparison of common volcanic rocks: Geological Society of America Bulletin, v. 86, p. 257-263.

Coats, R. R., 1956, Uranium and certain other trace elements in felsic volcanic rocks of Cenozoic age in the western U.S.: U.S. Geological Survey Professional Paper 300, p. 75-78.

Compton, R. B., 1962, Manual of field geology: New York, John Wiley and Sons, 378 p.

Crowe, B. M., 1978, Cenozoic volcanic geology and probable age of inception of basin-range faulting in the southeasternmost Chocolate Mountains, California: Geological Society of America Bulletin, v. 89, p. 251-264.

Davis, G. A., Evans, K. V., Frost, E., Lingrey, S. H., and Shackleford, T. J., 1977, Enigmatic Miocene low-angle faulting, southeastern California and west-central Arizona - Suprastructural tectonics?: Geological Society of America Abstracts with Programs, v. 9, p. 943-944.

Davis, G. H., and Coney, P. J., 1979, Geologic development of the Cordilleran metamorphic core complexes: Geology, v. 7, p. 120-124.

Deer, W. A., Howie, R. A., and Zussman, J., 1966, An introduction to the rock-forming minerals: London, Longmans, Green, and Company, 528 p.

Eaton, G. P., Peterson, D. L., Schumann, H. H., 1972, Geophysical, geohydrological, and geochemical reconnaissance of the Luke Salt Body, central Arizona: U.S. Geological Survey Professional Paper 753, 28 p.

Eberly, L. D., and Stanley, T. B., 1978, Cenozoic stratigraphy and geologic history of southwestern Arizona: Geological Society of America Bulletin, v. 89, p. 921-940.

Eichelberger, J. C., 1978, Andesitic volcanism and crustal evolution: Nature, v. 275, p. 21-27.

Elston, W. E., Rhodes, R. C., Coney, P. J., and Deal, E. G., 1976, Progress report on the Mogollon Plateau volcanic field, southwestern New Mexico, No. 3 - surface expression of a pluton, in Elston, W. E., and Northrop, S. A., eds., Cenozoic volcanism in southwestern New Mexico: New Mexico Geological Society Special Publication 5, p. 3-28.

Faure, Gunter, 1977, Principles of isotope geology: New York, Wiley and Sons, 464 p.

Fisher, R. V., 1960a, Criteria for recognition of laharic breccias, southern Cascade Mountains, Washington: Geological Society of America Bulletin, v. 71, p. 127-132.

_____1960b, Classification of volcanic breccias: Geological Society of America Bulletin, v. 71, p. 973-982.

_____1961, Proposed classification of volcaniclastic sediments and rocks: Geological Society of America Bulletin, v. 72, p. 1409-1414.
_____1966a, Mechanism of deposition from pyroclastic flows: American Journal of Science, v. 264, p. 350-363.
_____1966b, Rocks composed of volcanic fragments and their classification: Earth Science Review, v. 1, p. 287-298.
_____1971, Features of coarse-grained, high-concentration fluids and their deposits: Criteria for recognition of laharic breccias, southern Cascade Mountains, Washington: Geological Society of America Bulletin, v. 71, p. 127-132.
Folk, R. L., 1974, Petrology of sedimentary rocks: Austin, Texas, Hemphill Publishing, 182 p.
Fuis, G. S., 1974, The geology and mechanics of formation of the Fort Rock Dome, Yavapai County, Arizona: Pasadena, Calif., California Institute of Technology, Ph. D. dissertation, 154 p.
Gableman, J. W., 1977, Migration of uranium and thorium-exploration significance: American Association of Petroleum Geologists, Studies in Geology, no. 3, 168 p.
Gassaway, J. C., 1977, A reconnaissance study of Cenozoic geology in west-central Arizona: San Diego, Calif., San Diego State University, M.S. thesis, 120 p.
Gilluly, James, 1971, Plate tectonics and magmatic evolution: Geological Society of America Bulletin, v. 82, p. 2383-2396.
Gottfried, David, Annell, C. S., and Schwarz, L. J., 1977, Geochemistry of subsurface basalt from the deep corehole (Clubhouse Crossroads Corehole 1), near Charleston, South Carolina--Magma type and tectonic implications: U.S. Geological Survey Professional Paper 1028-G, p. 91-113.
Green, T. H., and Ringwood, A. E., 1968, Genesis of the calc-alkaline igneous rock suite: Contributions to Mineralogy and Petrology, v. 18, p. 105-162.
Hamblin, W. K., and Best, M. G., 1975, The geologic boundary between the Colorado Plateau and the Basin and Range province: Geological Society of America Abstracts with Programs, v. 7, p. 1097.
Heiken, Grant, 1972, Morphology and petrography of volcanic ashes: Geological Society of America Bulletin, v. 83, p. 1961-1988.
Hildreth, Wes, 1979, The Bishop Tuff--Evidence for the origin of compositional zonation in silicic magma chambers: Geological Society of America Special Paper 190, p. 43-75.
Hildreth, Wes, Grunder, A. L., and Drake, R. E., 1984, The Loma Seca Tuff and the Calabozos caldera: A major ash-flow and caldera complex in the southern Andes of central Chile: Geological Society of America Bulletin, v. 95, p. 45-54.
Hyndman, D. W., 1972, Petrology of igneous and metamorphic rocks: New York, McGraw-Hill Co., 533 p.
Irvine, T. N., and Baragar, W. R. A., 1971, A guide to the chemical classification of the common volcanic rocks: Canadian Journal of Earth Sciences, v. 8, p. 523-548.
Jakes, P., and White, A. J. R., 1972, Major and trace element abundances in volcanic rocks of orogenic areas: Geological Society of America Bulletin, v. 83, p. 29-40.
Johnson, R. W., 1976, Potassium variation across the New Britain volcanic arc: Earth and Planetary Science Letters, v. 31, p. 184-191.

Kane, M. F., Mabey, D. R., and Brace, R. L., 1976, A gravity and magnetic investigation of the Long Valley Caldera, Mono County, California: Journal of Geophysical Research, v. 81, no. 5, p. 754-762.
Karig, D. E., 1965, Geophysical evidence of a caldera at Bonanza, Colorado: U.S. Geological Survey Professional Paper 525-B, p. B9-B12.
Keith, S. B., 1978, Paleosubduction geometries inferred from Cretaceous and Tertiary magmatic patterns in southwestern North America: Geology, v. 6, p. 516-521.
Keith, S. B., Reynolds, S. J., and Rehrig, W. A., 1981, Relations of tectonics to ore deposits in the southern Cordillera; Field Trip no. 7: Arizona Geological Society, 114 p.
Kuno, Hisashi, 1959, Origin of Cenozoic petrographic provinces of Japan and surrounding areas: Bulletin Volcanologique, v. 20, p. 37-76.
Landes, K. K., 1959, Petroleum geology: New York, Wiley and Sons, 443 p.
Lasky, S. G., and Webber, B. N., 1949, Manganese resources of the Artillery Mountains region, Mohave County, Arizona: U.S. Geological Survey Bulletin 961, 86 p.
Leeman, W. P., and Rogers, J. J. W., 1970, Late Cenozoic alkali-olivine basalts of the Basin-Range province, U.S.A.: Contributions to Mineralogy and Petrology, v. 25, p. 1-24.
Lipman, P. W., 1965, Chemical comparison of glassy and crystalline volcanic rocks: U.S. Geological Survey Bulletin, 1201-D, p. 1-24.
_____1975, Evolution of the Platoro caldera complex and related volcanic rocks, southeastern San Juan Mountains, Colorado: U.S. Geological Survey Professional Paper 852, 128 p.
Lipman, P. W., Prostka, H. J., and Christiansen, R. L., 1971, Evolving subduction zones in the western United States, as interpreted from igneous rocks: Science, v. 174, p. 821-825.
Lucchitta, Ivo, 1978, The central Arizona Transition Zone--A Precambrian plate boundary?: Geological Society of America Abstracts with Programs, v. 10, p. 114.
MacDonald, G. A., 1972, Volcanoes: Englewood Cliffs, N.J., Prentice-Hall, 510 p.
Mackin, J. H., 1960, Eruptive tectonic hypothesis for origin of Basin-Range structure: Geological Society of America Abstracts with Programs, v. 71, p. 1921.
McBirney, A. R., and Williams, Howel, 1969, Geology and petrology of the Galapagos Islands: Geological Society of America Memoir 118, 197 p.
McKee, E. H., 1971, Tertiary igneous chronology of the Great Basin of western United States--implications for tectonic models: Geological Society of America Bulletin, v. 82, p. 3497-3502.
McKee, E. H., and Anderson, C. A., 1971, Age and chemistry of tertiary volcanic rocks in north-central Arizona and relation of the rocks to the Colorado Plateaus: Geological Society of America Bulletin, v. 82, p. 2767-2782.
McKee, E. H., Noble, D. C., and Silberman, M. L., 1970, Middle Miocene hiatus in volcanic activity in the Great Basin area of the western United States: Earth and Planetary Science Letters, v. 8, p. 93-96.
Miller, W. R., McHugh, J. B., and Ficklin, W. H., 1979, Possible uranium mineralization, Mineral Mountains, Utah: U.S. Geological Survey Open-File Report 79-1354, 44 p.
Moore, J. G., 1962, K/Na ratio of Cenozoic igneous rocks of the western United States: Geochimica et Cosmochimica Acta, v. 26, p. 101-130.

_____1967, Base surge in Recent volcanic eruptions: Bulletin Volcanologique, v. 30, p. 337-363.
Moore, J. G., Nakamura, K., and Alcaraz, A., 1966, The 1965 eruption of Taal Volcano: Science, v. 151, p. 955-960.
Moorhouse, W. W., 1959, The study of rocks in thin section: New York, Harper and Row, 514 p.
Noble, D. C., 1972, Some observations on the Cenozoic volcano-tectonic evolution of the Great Basin, western United States: Earth and Planetary Science Letters, v. 17, p. 142-150.
Nockolds, S. R., 1966, Average chemical compositions of some igneous rocks: Geological Society of America Bulletin, v. 65, p. 1007-1032.
Nockolds, S. R., Knox, R. W. O'B., and Chinner, G. A., 1978, Petrology: London, Cambridge University Press, 435 p.
Otton, J. K., 1977, Geology of uraniferous Tertiary rocks in the Artillery Peak-Date Creek Basin, west-central Arizona: U.S. Geological Survey Circular 753, p. 35-36.
_____1981, Geology and genesis of the Anderson Mine, a carbonaceous lacustrine uranium deposit, western Arizona: a summary report: U.S. Geological Survey Open-File Report 81-780.
Otton, J. K., and Brooks, W. E., 1978, Tectonic history of the Colorado Plateau margin, Date Creek Basin and adjacent areas, west-central Arizona [abs.], in Plateau Uplift: Mode and Mechanism: Lunar and Planetary Institute Contributions 329, p. 31-33.
Pakiser, L. C., 1961, Gravity, volcanism, and crustal deformation in Long Valley, California: U.S. Geological Survey Professional Paper 424-B, p. 250-253.
Pakiser, L. C., and Zietz, Isidore, 1965, Transcontinental crustal and upper mantle structure: Reviews of Geophysics, v. 3, p. 505-520.
Parsons, W. H., 1969, Criteria for the recognition of volcanic breccias--Review: Geological Society of America Memoir 115, p. 263-304.
Pearce, J. A., and Norry, M. J., 1979, Petrogenetic implications of Ti, Zr, Y, and Nb variations in volcanic rocks: Contributions to Mineralogy and Petrology, v. 69, p. 33-47.
Peccerillo, Angelo, and Taylor, S. R., 1976, Geochemistry of Eocene calc-alkaline volcanic rocks from the Kastamonu area, northern Turkey: Contributions to Mineralogy and Petrology, v. 58, p. 63-81.
Peirce, H. W., Shafiqullah, Mohammed, and Damon, P. E., 1978, Pre-Pliocene Tertiary erosion, deposition, faulting, and volcanism--Southern boundary of the Colorado Plateau--Arizona: Geological Society of America Abstracts with Programs, v. 10, p. 141.
Peterson, D. W., 1961, Flattening ratios of pumice fragments in an ash-flow sheet near Superior, Arizona: U.S. Geological Survey Professional Paper 424-D, p. 82-84.
Pettijohn, F. J., 1975, Sedimentary rocks: New York, Harper and Row, 628 p.
Plouff, Donald, and Pakiser, L. C., 1972, Gravity study of the San Juan Mountains, Colorado: U.S. Geological Survey Professional Paper 800-B, p. 183-190.
Potter, P. E., and Pettijohn, F. J., 1977, Paleocurrents and basin analysis: New York, Springer-Verlag, 425 p.
Ratté, J. C., and Grotbo, Terry, 1979, Chemical analyses and norms of 81 volcanic rocks from part of the Mogollon-Datil volcanic field, southwestern New Mexico: U.S. Geological Survey Open-File Report 79-1435, 35 p.

Rehrig, W. A., and Reynolds, S. J., 1977, A northwest zone of metamorphic core complexes in Arizona: Geological Society of America Abstracts with Programs, v. 9, p. 1139.

Rehrig, W. A., Shafiqullah, Mohammed, and Damon, P. E., 1980, Geochronology, geology, and listric normal faulting of the Vulture Mountains, Maricopa County, Arizona: Arizona Geological Society Digest, v. 12, p. 89-110.

Reineck, H-E., and Singh, I. B., 1975, Depositional sedimentary environments: New York, Springer-Verlag, 439 p.

Ringwood, A. E., 1975, Composition and petrology of the earth's mantle: New York, McGraw-Hill, 618 p.

Roper, M. W., and Wallace, A. B., 1981, Geology of the Aurora uranium prospect, Malheur County, Oregon, in Goodell, P. C., and Waters, A. C., eds., Uranium in volcanic and volcaniclastic rocks: American Association of Petroleum Geologists Studies in Geology, no. 13, 331 p.

Rose, W. I., and Bornhorst, T. J., 1981, Uranium and thorium in selected Quaternary volcanic rocks of Guatemala and Sumatra: Evidence for uranium distribution, in Goodell, P. C., and Waters, A. C., eds., Uranium in volcanic and volcaniclastic rocks: American Association of Petroleum Geologists Studies in Geology, no. 13, 331 p.

Rosholt, J. N., and Noble, D. C., 1969, Loss of uranium from crystallized silicic volcanic rocks: Earth and Planetary Science Letters, v. 6, p. 268-270.

Rytuba, J. J., and Glanzman, R. K., 1978, Relation of mercury, uranium, and lithium deposits to the McDermitt caldera complex, Nevada-Oregon: U.S. Geological Survey Open-File Report 78-926, 28 p.

Schmid, R., 1981, Descriptive nomenclature and classification of pyroclastic deposits and fragments: Geology, v. 9, p. 41-43.

Schmincke, H. U., 1967, Graded lahars in the type sections of the Ellensburg formation, south-central Washington: Journal of Sedimentary Petrology, v. 37, p. 438-448.

Shackelford, T. J., 1976, Structural geology of the Rawhide Mountains, Mohave County, Arizona: Los Angeles, Calif., University of Southern California, Ph. D. dissertation, 176 p.

Shafiqullah, Mohammed, Damon, P. E., Lynch, D. J., Reynolds, S. J., Rehrig, W. A., and Raymond, R. H., 1980, K-Ar geochronology and geologic history of southwestern Arizona and adjacent areas: Arizona Geological Society Digest, v. 12, p. 201-260.

Sherbourne, J. E., Buckovic, W. A., Dewitt, D. B., Hellinger, T. S., and Pavlak, S. J., 1979, Major uranium discovery in volcaniclastic sediments, Basin and Range province, Yavapai County, Arizona: American Association of Petroleum Geologists Bulletin, v. 63, p. 621-646.

Sheridan, M. F., Stuckless, J. S., and Fodor, R. V., 1970, A Tertiary silicic cauldron complex at the northern margin of the Basin and Range province, central Arizona, U.S.A.: Bulletin Volcanologique, v. 34, p. 649-662.

Smith, R. L., 1979, Ash-flow magmatism: Geological Society of America Special Paper 180, p. 5-27.

Smith, R. L., and Bailey, R. A., 1966, The Bandelier Tuff--A study of ash-flow cycles from zoned magma chambers: Bulletin Volcanologique, v. 29, p. 83-103.

Stauder, W., 1973, Mechanism and spatial distribution of Chilean earthquakes with relation to subduction of the oceanic plate: Journal of Geophysical Research, v. 78, p. 5033-5061.

Steven, T. A., and Lipman, P. W., 1976, Calderas of the San Juan volcanic field, southwestern Colorado: U.S. Geological Survey Professional Paper 958, 35 p.

Stuckless, J. S., and O'Neil, J. R., 1973, Petrogenesis of the Superstition-Superior volcanic area as inferred from strontium- and oxygen-isotope studies: Geological Society of America Bulletin, v. 84, p. 1987-1998.

Stuckless, J. S., and Sheridan, M. F., 1971, Tertiary volcanic stratigraphy in the Goldfield and Superstition Mountains, Arizona: Geological Society of America Bulletin, v. 82, p. 3235-3240.

Thompson, G. A., and Zoback, M. L., 1978, Geophysical comparison of Colorado Plateau with Basin and Range: Geological Society of America Abstracts with Programs, v. 10, p. 150.

Thorson, J. P., 1971, Igneous petrology of the Oatman District, Mohave County, Arizona: Santa Barbara, Calif., University of California, Ph. D. dissertation, 189 p.

Van Der Plas, L., and Tobi, A. C., 1965, A chart for judging the reliability of point counting results: American Journal of Science, v. 263, p. 87-90.

Walker, G. P. L., 1980, The Taupo pumice; product of the most powerful known (ultraplinian) eruption?: Journal of Volcanology and Geothermal Research, v. 8, p. 69-94.

Wallace, A. B., and Roper, M. W., 1981, Geology and uranium deposits along the northeastern margin, McDermitt Caldera Complex, Oregon, in Goodell, P. C., and Waters, A. C., eds., Uranium in volcanic and volcaniclastic rocks: American Association of Petroleum Geologists Studies in Geology, no. 13, 331 p.

Warren, D. H., 1969, A seismic-refraction survey of crustal structure in central Arizona: Geological Society of America Bulletin, v. 80, p. 257-282.

Washington, H. S., 1917, Chemical analyses of igneous rocks published from 1884 to 1913: U.S. Geological Survey Professional Paper 99, 1201 p.

Waters, A. C., 1978, Some uranium deposits associated with volcanic rocks, western United States: U.S. Department of Energy Publication RME-2049, 13 p.

West, R. E., and Sumner, J. S., 1973, Bouguer gravity anomaly map of Arizona: Tucson, Ariz., University of Arizona, Department of Geosciences.

Williams, Howel, and McBirney, A. R., 1979, Volcanology: San Francisco, Freeman, Cooper and Company, 397 p.

Williams, Howel, Turner, F. J., and Gilbert, C. M., 1954, Petrography: San Francisco, Freeman and Company, 406 p.

Wilson, E. D., 1962, A resume of the geology of Arizona: Arizona Bureau of Mines Bulletin 171, 140 p.

Wilson, E. D., Moore, R. T., and Cooper, J. R., 1969, Geologic map of Arizona: Arizona Bureau of Mines and U.S. Geological Survey.

Wynn, J. C., and Otton, J. K., 1978, Complete Bouguer gravity map and gravity model of the Date Creek Basin, Maricopa, Mohave, and Yavapai Counties, Arizona: U.S. Geological Survey Open-File Report 78-362, 2 p.

Young, R. A., 1978, Early Cenozoic uplift, erosion, and volcanism along the Colorado Plateau margin in southern Mohave County, Arizona: Geological Society of America Abstracts with Programs, v. 10, p. 155.

Young, R. A., and Brennan, W. J., 1974, Peach Springs Tuff--Its bearing on structural evolution of the Colorado Plateau and development of Cenozoic drainage in Mohave County, Arizona: Geological Society of America Bulletin, v. 85, p. 83-90.

APPENDIX A

Location of Samples

Field No.	Location		Quadrangle
	Latitude	Longitude	
E-100-77(K-Ar)	34°19'33"	113°05'37"	MM
E-101-77	34°10'33"	113°0'42"	DCR
E-113-77	34°22'16"	113°14'18"	MMSW
E-132-77	34°18'52"	113°10'33"	MMSW
E-137-77	34°20'45"	113°12'09"	MMSW
E-138-77	34°21'08"	113°12'01"	MMSW
E-145-78	34°22'15"	113°14'50"	MMSW
E-149-78	34°17'53"	113°09'53"	MMSW
E-156-78	34°16'23"	113°09'05"	MMSW
E-162-78	34°17'53"	113°11'36"	MMSW
E-166-78	34°18'53"	113°12'35"	MMSW
E-167-78(K-Ar)	34°19'12"	113°12'40"	MMSW
E-169-78	34°19'45"	113°14'30"	MMSW
E-170-78	34"19'33"	113°14'27"	MMSW
E-171-78	34°19'21"	113°12'15"	MMSW
E-173-78	34°10'45"	113°06'28"	DCR
E-174-78	34°14'01"	113°11'03"	DCRNW
E-177-78	34°20'17"	113°14'04"	MMSW
E-186-78	34°20'29"	113°13'27"	MMSW
E-191B(K-Ar)	34°00'56"	113°06'55"	DCRSE
E-191C	34°00'56"	113°06'55"	DCRSE
E-191D	34°01'40"	113°07'50"	DCRSW
E-191E	34°00'56"	113°06'55"	DCRSE
E-191F	34°00'56"	113°06'55"	DCRSE
E-203-79	34°14'27"	113°09'15"	DCRNW
E-204-79	34°13'39"	113°08'11"	DCRNW
E-205-79	34°14'03"	113°07'52"	DCRNW
E-210-79	34°13'39"	113°10'48"	DCRNW
E-211-79	34°20'27"	113°13'31"	MMSW
E-212-79	34°20'26"	113°13'45"	MMSW
E-219-81	34°19'22"	113°09'53"	MMSW

DCR - Date Creek Ranch 7 1/2'
DCRNW - Date Creek Ranch Northwest 7 1/2'
DCRSE - Date Creek Ranch Southeast 7 1/2'
DCRSW - Date Creek Ranch Southwest 7 1/2'
MM - Malpais Mesa 7 1/2'
MMSW - Malpais Mesa Southwest 7 1/2'